Extracellular ATP and CD39 Activate cAMP-Mediated Mitochondrial Stress Response to Promote Cytarabine Resistance in Acute Myeloid Leukemia

Article *in* Cancer Discovery · July 2020

DOI: 10.1158/2159-8290.CD-19-1008

CITATIONS
54

READS
102

33 authors, including:

Nesrine Aroua
Cancer Research Center of Toulouse
12 PUBLICATIONS **838** CITATIONS
SEE PROFILE

Estelle Saland
French Institute of Health and Medical Research
86 PUBLICATIONS **3,150** CITATIONS
SEE PROFILE

Mohsen Hosseini
University Health Network
26 PUBLICATIONS **1,320** CITATIONS
SEE PROFILE

Claudie Bosc
Northwestern University
22 PUBLICATIONS **1,288** CITATIONS
SEE PROFILE

RESEARCH ARTICLE

Extracellular ATP and CD39 Activate cAMP-Mediated Mitochondrial Stress Response to Promote Cytarabine Resistance in Acute Myeloid Leukemia

Nesrine Aroua[1,2], Emeline Boet[1,2], Margherita Ghisi[1,2], Marie-Laure Nicolau-Travers[1,2,3], Estelle Saland[1,2], Ryan Gwilliam[1,2], Fabienne de Toni[1,2], Mohsen Hosseini[1,2], Pierre-Luc Mouchel[1,2,3], Thomas Farge[1,2], Claudie Bosc[1,2], Lucille Stuani[1,2], Marie Sabatier[1,2], Fetta Mazed[4,5], Clément Larrue[1,2], Latifa Jarrou[1,2], Sarah Gandarillas[6], Massimiliano Bardotti[6], Muriel Picard[2,7], Charlotte Syrykh[1,2,8], Camille Laurent[1,2,8], Mathilde Gotanègre[1,2], Nathalie Bonnefoy[9], Floriant Bellvert[10], Jean-Charles Portais[10], Nathalie Nicot[11], Francisco Azuaje[12], Tony Kaoma[12], Carine Joffre[1,2], Jérome Tamburini[4,5], Christian Récher[1,2,3], François Vergez[1,2,3], and Jean-Emmanuel Sarry[1,2]

ABSTRACT

Relapses driven by chemoresistant leukemic cell populations are the main cause of mortality for patients with acute myeloid leukemia (AML). Here, we show that the ectonucleotidase CD39 (ENTPD1) is upregulated in cytarabine-resistant leukemic cells from both AML cell lines and patient samples *in vivo* and *in vitro*. CD39 cell-surface expression and activity is increased in patients with AML upon chemotherapy compared with diagnosis, and enrichment in CD39-expressing blasts is a marker of adverse prognosis in the clinics. High CD39 activity promotes cytarabine resistance by enhancing mitochondrial activity and biogenesis through activation of a cAMP-mediated adaptive mitochondrial stress response. Finally, genetic and pharmacologic inhibition of CD39 ecto-ATPase activity blocks the mitochondrial reprogramming triggered by cytarabine treatment and markedly enhances its cytotoxicity in AML cells *in vitro* and *in vivo*. Together, these results reveal CD39 as a new residual disease marker and a promising therapeutic target to improve chemotherapy response in AML.

SIGNIFICANCE: Extracellular ATP and CD39–P2RY13–cAMP–OxPHOS axis are key regulators of cytarabine resistance, offering a new promising therapeutic strategy in AML.

[1]Centre de Recherches en Cancérologie de Toulouse, UMR1037 Inserm/Université Toulouse III-Paul Sabatier, ERL5294 CNRS, Equipe Labellisée LIGUE 2018, Toulouse, France. [2]University of Toulouse, Toulouse, France. [3]Service d'Hématologie, Institut Universitaire du Cancer de Toulouse-Oncopole, CHU de Toulouse, Toulouse, France. [4]Institut Cochin, Département Développement, Reproduction, Cancer, UMR8104-CNRS, U1016-INSERM, Paris. [5]Translational Research Centre in Onco-Hematology, Faculty of Medicine, University of Geneva, Geneva, Switzerland. [6]Centre Régional d'Exploration Fonctionnelle et Ressources Expérimentales, Service d'Expérimentation Animale, UMS006, Inserm, Toulouse, France. [7]Intensive Care Unit, Institut Universitaire du Cancer de Toulouse-Oncopole, CHU de Toulouse, Toulouse, France. [8]Service d'Anatomopathologie, Institut Universitaire du Cancer de Toulouse-Oncopole, CHU de Toulouse, Toulouse, France. [9]Institut de Recherche en Cancérologie de Montpellier, U1194, Inserm, Université de Montpellier, Institut régional du Cancer de Montpellier, Montpellier, France. [10]TBI, Université de Toulouse, CNRS, INRA, INSA, Toulouse, France. [11]LuxGene, Quantitative Biology Unit, Luxembourg Institute of Health, Luxembourg, Luxembourg. [12]Computational Biomedicine Research Group, Quantitative Biology Unit, Luxembourg Institute of Health, Luxembourg, Luxembourg.

Note: Supplementary data for this article are available at Cancer Discovery Online (http://cancerdiscovery.aacrjournals.org/).

N. Aroua, E. Boet, and M. Ghisi (listed in alphabetical order) share first co-authorship of this article.

Corresponding Author: Jean-Emmanuel Sarry, Inserm, U1037, Centre de Recherches en Cancérologie de Toulouse, F-31024 Toulouse cedex 3, France. Phone: 335-8274-1632; Fax: 335-6274-4558; E-mail: jean-emmanuel.sarry@inserm.fr

Cancer Discov 2020;10:1544–65

doi: 10.1158/2159-8290.CD-19-1008

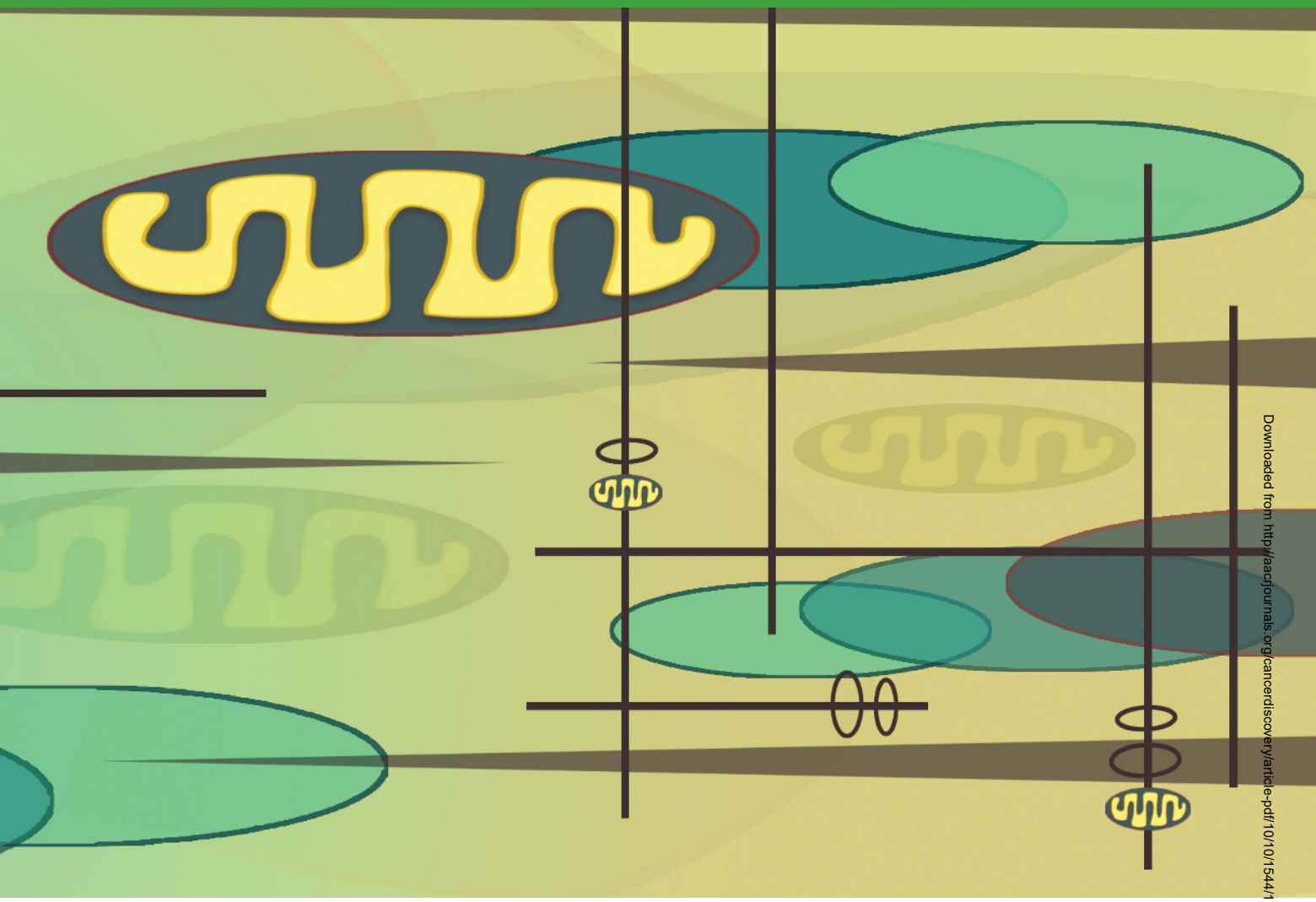

INTRODUCTION

Chemotherapy resistance is the major therapeutic barrier in acute myeloid leukemia (AML), the most common acute leukemia in adults. AML is characterized by clonal expansion of immature myeloblasts and initiates from rare leukemic stem cells (LSC). Despite a high rate of complete remission after conventional first-line induction chemotherapy [e.g., daunorubicin or idarubicin plus cytarabine (AraC)], the long-term prognosis is very poor for patients with AML. To date, the 5-year overall survival is still about 30% to 40% in patients younger than 60 years old and less than 20% in patients older than 60. This results from the high frequency of distant relapses (50% and 85% for patients younger and older than 60 years of age, respectively) caused by tumor regrowth initiated by chemoresistant leukemic clones (RLC) and characterized by a refractory phase during which no other treatment has shown any efficacy thus far (1, 2). Even with recent efficient targeted therapies that are FDA-approved or under clinical development, therapy resistance remains the major therapeutic barrier in AML. Therefore, understanding the molecular and cellular mechanisms driving chemoresistance is crucial for the development of new treatments eradicating RLCs and to improve the clinical outcome of these patients.

The biological basis of therapeutic resistance (drug efflux, detoxification enzymes, inaccessibility of the drug to the leukemic niche) currently represents an active area of research. However, the molecular mechanisms underlying AML chemoresistance are still poorly understood, especially *in vivo*. It is nevertheless increasingly recognized that the causes of chemoresistance and relapse reside within a small cell subpopulation within the bulk of leukemic cells. Supporting this view, clinical studies have shown that the presence of high levels of $CD34^{+}CD38^{lo/-}CD123^{+}$ cells at diagnosis correlates with adverse outcome in patients with AML in terms of response to therapy and overall survival (3, 4). Consistent with these data, Ishikawa and colleagues (5) have observed that this population is also the most resistant to cytarabine treatment *in vivo*. As a first step toward successful therapeutic eradication of these RLCs, it is now necessary to comprehensively profile the intrinsic and acquired characteristics of this cell population. We have recently established a powerful preclinical model to screen *in vivo* responses to conventional genotoxics and to mimic the chemoresistance and minimal residual disease observed in patients with AML after chemotherapy (6).

Accordingly, we have fully analyzed the response to chemotherapy of leukemic cells in AraC-treated AML patient-derived xenograft (PDX) mouse models. Surprisingly, we have found that cytarabine treatment equally kills both cycling and quiescent cells and does not necessarily lead to LSC enrichment *in vivo*. However, we observed that cytarabine chemoresistant leukemic cells exhibit elevated oxidative phosphorylation (OxPHOS) activity and that targeting mitochondrial oxidative metabolism with OxPHOS inhibitors sensitizes resistant AML cells to AraC (6, 7). Consistent with our findings, several groups have also demonstrated that essential mitochondrial functions contribute to resistance to multiple treatments in other cancer types (8–11).

Hyperleukocytosis is a clinical condition observed in patients with AML, which may lead to life-treatening complications such as leukostasis and is associated with a higher risk of relapse. Importantly, this condition is sustained by several mediators of inflammation, which were also reported to contribute to chemoresistance in AML (12–14). Supporting this idea, a recent study reported that inhibition of the inflammatory chemoresistance pathway with dexamethasone improved outcome of patients with AML (15). In line with these observations, recent work from our group (6) has highlighted a gene signature associated with the immune and inflammatory response after AraC treatment of PDX models *in vivo*. Among immune response mechanisms, the adenosine signaling pathway is one of the most prominent in cancer. CD39/ENTPD1 (ectonucleoside triphosphate diphosphohydrolase-1) is a member of the family of ectonuclotidases present on the outer surface of cells and a key component of the adenosine pathway. Together with CD73, CD39 catalyzes hydrolysis of extracellular adenosine triphosphate (eATP) and adenosine diphosphate (ADP) to produce adenosine, a recognized immunosuppressive molecule (16, 17). Therefore, CD39 has a critical role in tumor immunosurveillance and inflammatory response. Furthermore, although other nucleoside triphosphate diphosphohydrolases (NTPDases) exist, CD39 appears to be the main NTPDase in T lymphocytes and regulatory T cells (18). Recent lines of evidence have revealed high expression and activity of CD39 in several blood and solid tumors (such as head and neck cancer, thyroid cancer, colon cancer, pancreatic cancer, kidney cancer, testis cancer, and ovarian cancer), implicating this enzyme in promoting tumor growth and infiltration (19), and CD39 blockade was recently shown to enhance anticancer combination therapies in preclinical mouse models of solid tumors (20). Furthermore, CD39 is frequently detected in primary tumor cells, including AML blasts, cancer-derived exosomes, and tumor-associated endothelial cells. Notably, CD39 was reported to contribute to the immunosuppressive microenvironment in AML (21), while extracellular nucleotides (ATP, UTP) can inhibit AML homing and engraftment in NSG mice (22).

In this study, we employed computational analysis of transcriptomic datasets obtained from PDX models treated with cytarabine and primary patient samples to identify new druggable and relevant cell-surface proteins specifically expressed by RLCs. Among these genes, we uncovered CD39/ENTPD1 and confirmed that CD39 expression and activity are increased in residual AML cells post-chemotherapy *in vitro, in vivo*, and in the clinical setting. Herein, we have also shown that high CD39-expressing resistant AML cells rely on an enhanced mitochondrial metabolism and are strongly dependent on the coordinated induction of cAMP-PKA and ROS/ATF4 signaling downstream of CD39 to survive to chemotherapy. Accordingly, targeting CD39 markedly enhanced cytarabine cytotoxicity in AML cell lines and primary patient samples *in vitro* and *in vivo* through the inhibition of mitochondrial OxPHOS function, and this effect could be mimicked by inhibition of the PKA pathway. Overall, this work shows that a key mechanism of resistance to AraC involves CD39-dependent cross-talk between the energetic niche and leukemic mitochondrial functions through the CD39–P2RY13–cAMP–PKA axis in AML.

RESULTS

Enhanced CD39/ENTPD1 Expression and Activity Are Involved in Early Resistance to Cytarabine in AML

To identify new potential therapeutic targets involved in the onset of cytarabine resistance *in vivo*, we analyzed a previously identified signature of 68 genes that are significantly upregulated in residual AML cells from PDXs upon cytarabine treatment *in vivo* (ref. 6; GSE97393). Bioinformatic analysis of this specific gene signature showed an enrichment in several key cancer and immune response signaling pathways, including 8 genes involved in the inflammatory response (Supplementary Fig. S1A). As inflammation has been previously shown to play a critical role in the development of chemoresistance and to be linked to a poor prognosis in AML (15), we focused on this latter group of genes. Within this subset, we identified five genes encoding plasma membrane proteins sensitive to existing inhibitors, thus representing relevant druggable targets of RLCs *in vivo*. Importantly, two of these genes, *ENTPD1* (*CD39*) and the fatty-acid translocase *CD36*, were specifically overexpressed in AML cells compared with normal hematopoietic stem cells, highlighting their potential as therapeutic targets (Supplementary Fig. S1B and S1C). As CD36 has already been shown by our group and other groups to be a prognostic marker in myeloid leukemia (6, 23–25), we focused on CD39. The ecto-ATPase (eATPase) CD39 is well known for its immunosuppressive and proangiogenic function in multiple cancer types (16, 17). However, its role in AML cells and its contribution to AML chemoresistance are currently unknown.

Our gene expression data indicated that CD39 expression was upregulated in residual AML cells upon cytarabine treatment. To confirm that enhanced transcription correlated with increased surface protein levels, we studied CD39 cell-surface expression in residual viable AML cells from the bone marrow of 36 PDXs (Supplementary Table S1) following treatment with cytarabine (representative flow plot in Supplementary Fig. S2A). As expected, we observed a significant cytoreduction of the total cell tumor burden in the bone marrow and spleen (26 PDXs treated with 60 mg/kg/day of cytarabine; Fig. 1A; Supplementary Fig. S2B and S2C; 10 PDXs treated with 30 mg/kg of cytarabine; Supplementary Fig. S2D and S2E) of these different PDX models upon cytarabine treatment *in vivo*. In line with our gene expression data, despite a certain level of interpatient variability, we observed in the majority of

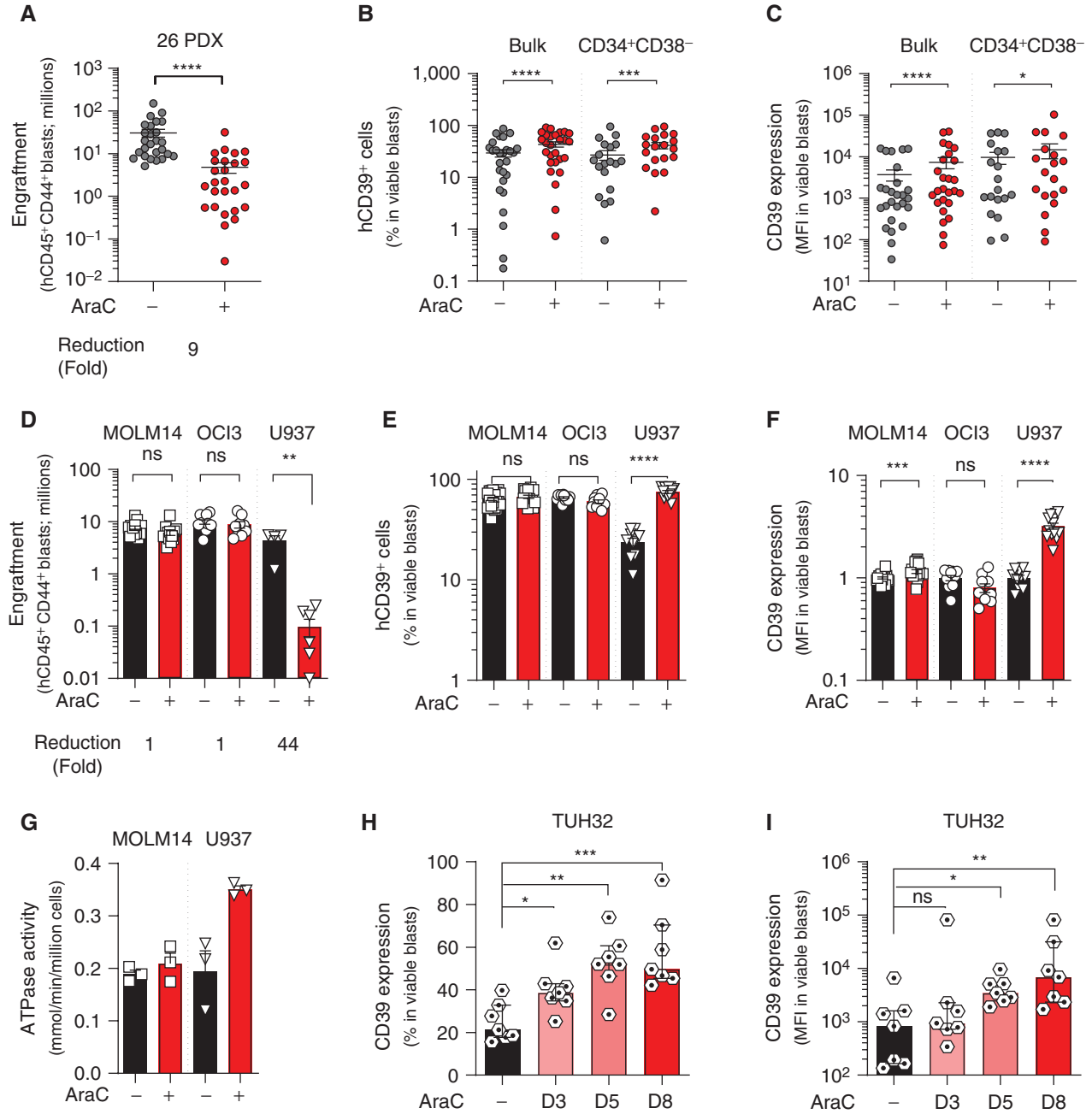

Figure 1. Identification of the ectonucleotidase CD39/ENTPD1 as a new actor of early resistance to cytarabine (AraC) in AML. **A,** The total cell tumor burden in cytarabine-treated compared with PBS-treated xenografted mice is shown for 26 PDXs. The total cell tumor burden was quantified using flow cytometry as the total number of human CD45+/CD33+/CD44+ AML blasts in the bone marrow and spleen of the xenografted mice. **B** and **C,** The percentage (**B**) and MFI (**C**) of CD39+ cells in the bulk population and in the CD34+CD38− immature subpopulation of human viable residual CD45+CD33+ AML cells was assessed in the bone marrow of cytarabine-treated compared with PBS-treated xenografted mice by flow cytometry. The result from 26 PDXs is shown. **D–F,** Flow cytometry analysis of xenografts (CLDX) derived from two cytarabine-resistant AML cell lines (MOLM14, OCI-AML3) and one sensitive AML cell line (U937) to assess, respectively, (**D**) the total tumor cell burden in bone marrow and spleen of human viable AML cells in cytarabine- and PBS-treated CLDXs, (**E**) the percentage of CD39+ AML cells, and (**F**) the CD39 MFI in AML cells from the bone marrow of the xenografted mice. In **F,** the relative increase in CD39 MFI in AML cells recovered from cytarabine-treated versus vehicle-treated xenografted mice is shown. For the purpose of the analysis, the MFI value of one xenograft from the control group was put equal to 1. **G,** The eATPase activity was assessed in MOLM14 and U937 CLDX models 3 days after the end of cytarabine or vehicle treatment. The concentration of nonhydrolyzed extracellular ATP was determined using the ATPlite assay (PerkinElmer). **H** and **I,** Flow cytometric analysis of human CD45+CD33+ residual AML cells harvested from the bone marrow of xenografted mice at day 3, 5, and 8 after the start of cytarabine treatment compared with untreated xenografted mice. The expression level of CD39 was quantified as percentage of CD39-expressing AML cells (**H**) and MFI of CD39 in the total viable AML population (**I**). *, $P \le 0.05$; **, $P \le 0.01$; ***, $P \le 0.001$; ****, $P \le 0.0001$; ns, not significant.

our PDXs an increase both in the percentage of CD39-positive cells and in the intensity of CD39 expression in the bulk residual AML population as well as in the immature $CD34^+CD38^-$ residual cell subpopulation in cytarabine-treated compared with vehicle-treated xenografted mice (Fig. 1B and C; Supplementary Fig. S2B–S2E). We then investigated the expression of CD39 in our panel of cell line–derived xenografted (CLDX) models characterized by different levels of sensitivity to AraC *in vivo* (6) and *in vitro* (representative gating strategy for *in vivo* and *in vitro* experiments, respectively, in Supplementary Fig. S3A and S3B). Although AraC treatment resulted in the induction of cell death in the four AML cell lines tested (HL60, MOLM14, U937, and KG1a; Supplementary Fig. S3C), changes in the transcript and the cell-surface expression of CD39 were significant but variable across these AML cell lines *in vitro* (Supplementary Fig. S3D–S3F). While MOLM14 and OCI-AML3 CLDX models are highly resistant to AraC chemotherapy *in vivo*, the U937 model is more sensitive and initially responds well to the treatment (total cell tumor burden fold reduction greater than 10 in cytarabine- vs. PBS-treated mice; Fig. 1D). The majority (~70%) of the intrinsically resistant MOLM14 and OCI-AML3 cells expressed CD39 *in vivo*. In contrast, only a small fraction (~30%) of U937 cells expressed CD39. Interestingly, we observed a significant increase in the percentage of CD39-positive cells as well as the intensity of CD39 cell-surface expression (Fig. 1E and F; Supplementary Fig. S3G), associated with an increase in CD39 eATPase activity (Fig. 1G) in residual U937 cells surviving post chemotherapy, whereas no or minimal change in CD39 expression and activity was detected in MOLM14 and OCI-AML3 cells (Fig. 1E–G; Supplementary Fig. S3G).

Next, we studied the kinetics of upregulation of CD39 in RLCs *in vivo*, during cytarabine treatment (day+3), immediately after the last dose of cytarabine treatment (day+5), and at day+8 in AML-xenografted NSG mice. Starting from day+5, we observed the appearance of RLCs with an increased CD39 expression (Fig. 1H and I). Of note, CD39-positive cells were not decreased at day 3 (Fig. 1H and I), and selection for CD39-positive cells occurred without genetic and mutational changes over time, as major founder mutations were present at diagnosis in patients and in the PDX throughout the same time course (Supplementary Fig. S4A). Altogether, these data strongly suggest that the CD39-positive phenotype may preexist before xenotransplantation and chemotherapy, and be selected and enhanced by cytarabine treatment *in vivo*. To test this hypothesis, we assessed whether sorted $CD39^{hi}$ and $CD39^{lo}$ cell subpopulations had a differential sensitivity to cytarabine treatment. We first sorted $CD39^{hi}$ and $CD39^{lo}$ fractions from therapy-naïve AML cells from MOLM14 and U937 AML cell lines *in vitro* (Supplementary Fig. S4B). Although the proliferation rate and cell-cycle status were similar in the two cellular subsets (Supplementary Fig. S4C and S4D), both MOLM14 and U937 $CD39^{hi}$ fractions showed a significantly higher IC_{50} for cytarabine compared with their respective $CD39^{lo}$ counterparts (Supplementary Fig. S4E and S4F). This diminished sensitivity to cytarabine of the $CD39^{hi}$ cell subset was confirmed on FACS-purified $CD39^{hi}$ and $CD39^{lo}$ AML fractions obtained *ex vivo* from both CLDXs and PDXs (Supplementary Fig. S4G). Interestingly, this differential sensitivity of the $CD39^{hi}$ and $CD39^{lo}$ cells was specific to cytarabine because we did not observe any significant difference in the induction of cell death in the two cell subsets upon treatment with idarubicin or venetoclax (ABT-199; Supplementary Fig. S4H).

Overall, our data indicate that a $CD39^{hi}$ phenotype characterizes *in vitro* and *in vivo* a subset of AML cells with a higher intrinsic resistance to cytarabine treatment. Importantly, this phenotype preexists and is amplified upon cytarabine chemotherapy *in vivo*.

Identification of CD39/ENTPD1 as a New Prognostic Marker Associated with Poor Response to Chemotherapy in Patients with AML

To evaluate the clinical relevance of our findings, we analyzed the expression of CD39 in patients with AML. Analysis of a cohort of 162 patients with AML at diagnosis indicated heterogeneous expression of CD39 (Fig. 2A). The expression of CD39 was not associated with the presence of specific recurrent mutations in AML (Supplementary Fig. S5A). However, we observed a correlation between CD39 cell-surface expression and FAB classification with a lower level of expression associated with the most undifferentiated AML subtypes (Supplementary Fig. S5B). This observation was also supported by the analysis of publicly available gene expression datasets from patients with AML (Supplementary Fig. S5C and S5D).

We then followed 98 of these patients comparing CD39 cell-surface expression at diagnosis and at day 35 (D35) after intensive chemotherapy. In accordance with our preclinical model, we showed a significant tumor reduction or complete remission in most of the patients after treatment (Fig. 2B), and demonstrated an overall increase in the percentage of CD39-positive cells in the residual blasts from those patients at day 35 post–intensive chemotherapy (Fig. 2C). We then stratified these patients with AML based on their fold enrichment in CD39-expressing cells upon chemotherapy in respect to diagnosis (CD39 was considered enriched with D35 vs. diagnosis fold change > 1.25, cutoff higher than the technical coefficient of variation for FACS). This defined a group of "high CD39 ratio" ($n = 74$) and "low CD39 ratio" patients ($n = 24$; Fig. 2D). Strikingly, the "high CD39 ratio" patients displayed a significantly worse disease-free survival compared with the "low CD39 ratio" group (Fig. 2E). This survival disadvantage was even more evident when focusing on the group of patients younger than 60 years of age (Fig. 2F). Finally, we investigated whether CD39-positive cell expansion upon chemotherapy could further stratify patients classified in favorable, intermediate, and high cytogenetic risk groups (Supplementary Fig. S6A). The increase in CD39-positive cells did not significantly improve the prognostic classification of intermediate and high cytogenetic risk patients (Supplementary Fig. S6B and S6C). However, this analysis revealed that patients with AML from the favorable cytogenetic risk subgroup, but characterized by a marked increase in CD39-expressing cells upon chemotherapy, displayed a significantly higher rate of short-term relapse and poorer clinical outcome (Fig. 2G).

Overall, these findings highlight the clinical relevance of our results obtained in PDXs and CLDXs and define CD39 as a marker of minimal residual disease and adverse prognosis in patients with AML.

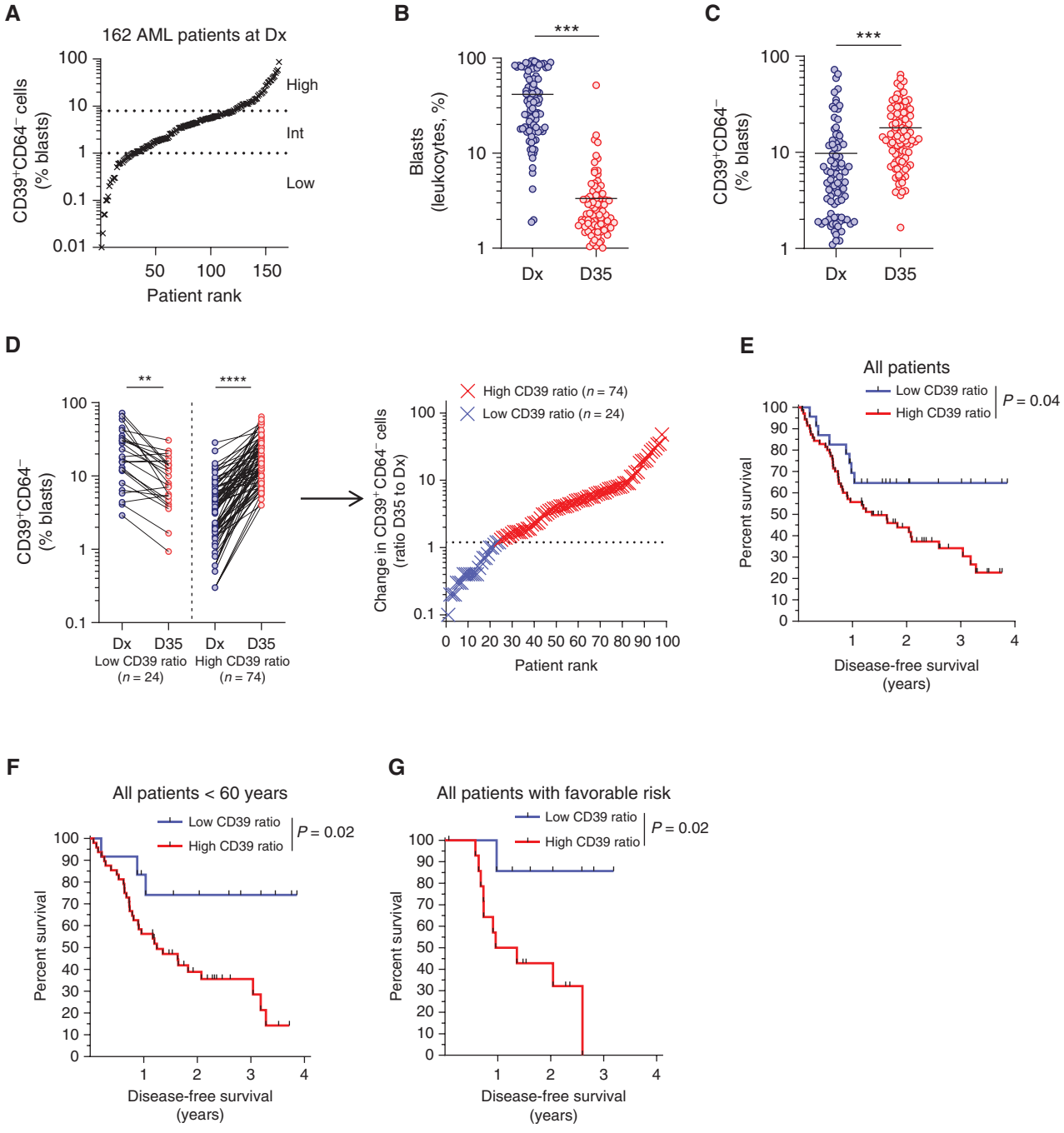

Figure 2. CD39 is a new prognostic marker associated with poor response to chemotherapy in patients with AML. **A,** Flow cytometric analysis of the percentage of $CD39^+CD64^-$ blasts in the peripheral blood of 162 patients with AML at diagnosis (Dx). **B** and **C,** Flow cytometric analysis of the percentage of total blasts (**B**) and $CD39^+CD64^-$ blasts (**C**) in the peripheral blood of 98 patients with AML obtained at diagnosis (Dx) and at 35 days post chemotherapy (D35). **D,** Distribution of the patients based on the fold-change enrichment in the % of $CD39^+CD64^-$ blasts at day 35 versus diagnosis. Patients with a D35 versus diagnosis fold change > 1.2 were classified as "High CD39 ratio," whereas patients with a fold change ≤ 1.2 were classified as "Low CD39 ratio." On left, the % of $CD39^+CD64^-$ blasts at diagnosis and D35 for each individual patient in the high (74 patients) and low (24 patients) CD39 ratio group is shown. The values at diagnosis and D35 for the same patient are connected by a line. **E–G,** Disease-free survival analysis on the basis of the fold-change enrichment in the percent of $CD39^+CD64^-$ blasts post chemotherapy compared with diagnosis, respectively, on the entire cohort of patients with AML ($n = 98$; **E**), on the subgroup of patients younger then 60 years of age ($n = 60$; **F**) and on the subgroup of patients classified as "Favorable risk" based on the European Leukemia Net (ELN) genetic-risk classification ($n = 23$; **G**).

CD39 Expression Is Associated with Higher Mitochondrial Activity and Biogenesis

As previous studies have demonstrated that drug-resistant AML cells exhibit high OxPHOS function and gene signatures *in vivo* (6, 9, 10), we investigated whether an OxPHOS gene signature was enriched in the transcriptomes of AML cells with high CD39 expression. We confirmed a positive correlation between *CD39* RNA expression and our previously defined "high OxPHOS" gene signature (6), making use of two independent transcriptomic databases from patients with AML that we stratified as $CD39^{lo}$ and $CD39^{hi}$ [GSE97393: NES = −1.84, FDRq < 0.001 and The Cancer Genome Atlas (TCGA): NES = −1.50, FDRq = 0.004, respectively; Fig. 3A; Supplementary Fig. S7A]. We then compared the metabolic status and mitochondrial activity of primary AML cells from patients with high or low levels of CD39 expression (Supplementary Fig. S7B and S7C). Primary cells from patients with $CD39^{hi}$ AML displayed on average increased eATPase activity compared with $CD39^{lo}$ patients (Fig. 3B), and this was associated with a modest increase in mitochondrial membrane potential (MMP) and a larger increase in basal oxygen consumption rate (OCR; Fig. 3C and D). We then sorted the low and high CD39 cell fractions from one of our PDXs (TUH10) after treatment *in vivo* with cytarabine or PBS (Supplementary Fig. S7D). In line with our previous results on the primary patient samples, the *ex vivo* analysis of the metabolic status and OCR of the two cell subsets showed increased basal, maximal uncoupler-stimulated respiration and ATP-linked respiration in $CD39^{hi}$ AML cellular subsets (Fig. 3E; Supplementary Fig. S7E–S7H). This was coupled with an augmented extracellular acidification rate (ECAR) linked to glycolysis, suggesting a global enhancement of cellular energetic capacity (Supplementary Fig. S7I and S7J) in $CD39^{hi}$ fractions compared with $CD39^{lo}$ fractions from PBS-treated mice. In accordance with our previously published data (6), cytarabine treatment resulted in the selection of residual viable AML cells with substantially increased basal and maximal uncoupler-stimulated OCR as well as ATP-linked OCR (Fig. 3E; Supplementary Fig. S7E–S7H). Overall, this indicated that increased levels of CD39 were associated with an enhanced mitochondrial activity and OxPHOS function in AML cells, which we previously identified as a feature of cytarabine-resistant AML cells.

To specifically study the direct effect of modulating CD39 expression on AML cell metabolism, we transduced the AML cell line MOLM14 with viral vectors expressing two different shRNAs targeting CD39. Transduction of MOLM14 with the sh*CD39*-expressing lentiviral vectors resulted in efficient silencing of the ectonucleotidase both at the mRNA level and at the protein level (Supplementary Fig. S8A and S8B), leading to a significant downregulation of the expression of this marker at the cell surface (Supplementary Fig. S8C). Silencing of CD39 resulted in a dramatic decrease in both basal and ATP-linked OCR in MOLM14 (Fig. 3F–H), which translated into a reduced generation of mitochondrial-derived ATP (Fig. 3I). This decreased mitochondrial OxPHOS activity was associated with a reduced expression of subunits of the electron transport chain (ETC) complexes and of well-known effectors of mitochondrial biogenesis (i.e., NRF1, PGC1α; Fig. 3J). Overall, these results indicate that CD39 positively controls mitochondrial function and OxPHOS, at least in part, by controlling the expression of the key transcriptional activators NRF1 and PGC1α promoting mitochondrial biogenesis.

Pharmacologic Inhibition of CD39 Ectoducleotidase Activity Inhibits the Metabolic Reprogramming Associated with Cytarabine Resistance and Enhances AML Cell Sensitivity to Cytarabine *In Vitro*

Next, we sought to determine whether inhibition of CD39 activity by polyoxometalate 1 (POM1), a pharmacologic inhibitor of nucleoside triphosphate diphosphohydrolase activity (26), could inhibit the metabolic reprogramming triggered by cytarabine and sensitize AML cells to the chemotherapeutic treatment *in vitro* (Fig. 4A). As expected, POM1 inhibited the increase of the CD39 eATPase activity upon cytarabine treatment in all AML cell lines tested *in vitro* (MOLM14, OCI-AML3, MV4-11; Fig. 4B; Supplementary Fig. S8D), leading to an accumulation of eATP in the medium (MOLM14; Supplementary Fig. S8E). Accordingly, inhibition of CD39 by POM1 in MOLM14 abrogated the expansion of the extracellular ADP and AMP pools triggered by cytarabine (Supplementary Fig. S8E). Furthermore, POM1 treatment repressed the cytarabine-induced increase in basal OCR, mitochondrial mass, mitochondrial DNA (mtDNA) level, and the protein level of ETC subunits (Fig. 4C–F; Supplementary Fig. S8F–S8I). Importantly, POM1 treatment significantly enhanced the loss of mitochondrial membrane potential (Fig. 4G; Supplementary Fig. S8J) and the induction of apoptosis (Fig. 4H; Supplementary Fig. S8K) triggered by cytarabine treatment *in vitro* in all three AML cell lines tested.

Figure 3. CD39 controls mitochondrial function and biogenesis. **A,** Gene set enrichment analysis (GSEA) of high OxPHOS gene signature (from ref. 6) was performed from transcriptomes of patients with AML classified as CD39 high versus low based on the level of *CD39* mRNA expression in (GSE97393; ref. 6) and TCGA cohorts. **B–D,** Viable AML blasts were purified by FACS-sorting from primary AML samples. The primary samples were classified into CD39 low and high based on the percent of CD39-expressing blasts (Supplementary Fig. S7B; the median was used as cut-off value). Next, the eATPase activity (**B**), as well as the OxPHOS status of the $CD39^{hi}$ versus $CD39^{lo}$ primary AML samples was analyzed *ex vivo* (**C** and **D**). The mitochondrial membrane potential (MMP) was assessed by flow cytometry using a TMRE probe (**C**) and the oxygen consumption rate (OCR; basal oxygen consumption rate is shown) was assessed by Seahorse (**D**). **E,** OCR of PDX-derived AML cells (TUH10) obtained from leukemic mice pretreated *in vivo* with cytarabine (AraC; 60 mg/kg/day) or with vehicle for 5 days. $CD33^{+}CD44^{+}$ AML cells were FACS-sorted on the basis of CD39 expression 3 days after the end of the *in vivo* treatment and the OCR of $CD39^{hi}$ and $CD39^{lo}$ subsets was assessed *ex vivo* by Seahorse assay. **F–I,** OCR (including basal oxygen consumption rate and ATP-linked oxygen consumption; **F–H**) and mitochondrial ATP production (**I**) was assessed, respectively, using a Seahorse analyzer and Promega Cell Titer-Glo kit for MOLM14 cells transduced with lentiviral vectors expressing either control (shCTL.1 and shCTL.2) or anti-CD39 (sh*CD39*.3 and sh*CD39*.4) shRNAs *in vitro*. **J,** Protein expression of the OxPHOS mitochondrial complexes, as well as of the transcription factors PGC1α, NRF1, and TFAM was assessed by Western blot analysis in MOLM14 cells expressing anti-CD39 or control shRNAs *in vitro*. The graph on the right shows densitometric quantification of Western blot bands normalized by the housekeeping gene β-actin and relative to the average of the shCT (shCT.1 and shCT.2) samples. *, $P \le 0.05$; **, $P \le 0.01$; ***, $P \le 0.001$.

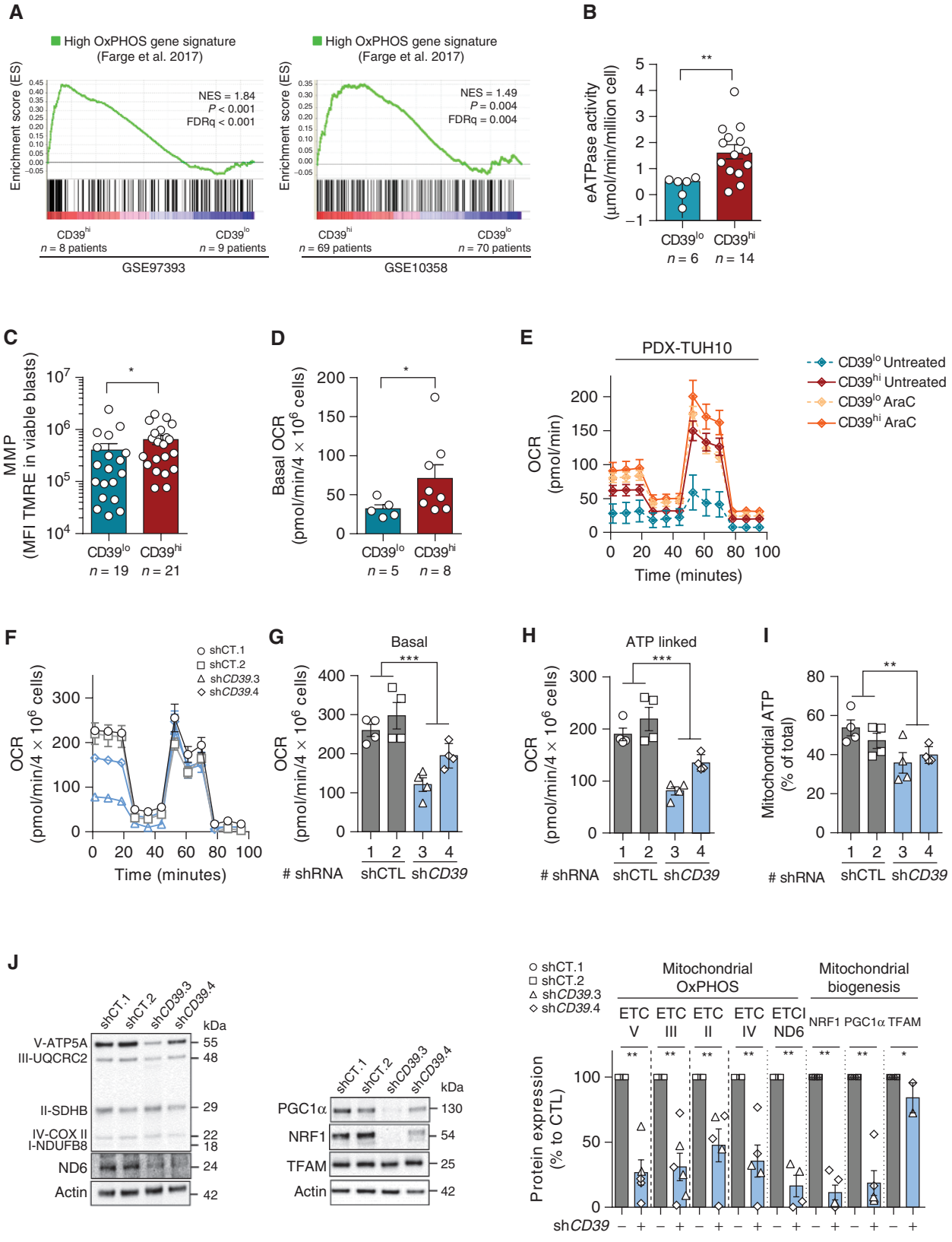

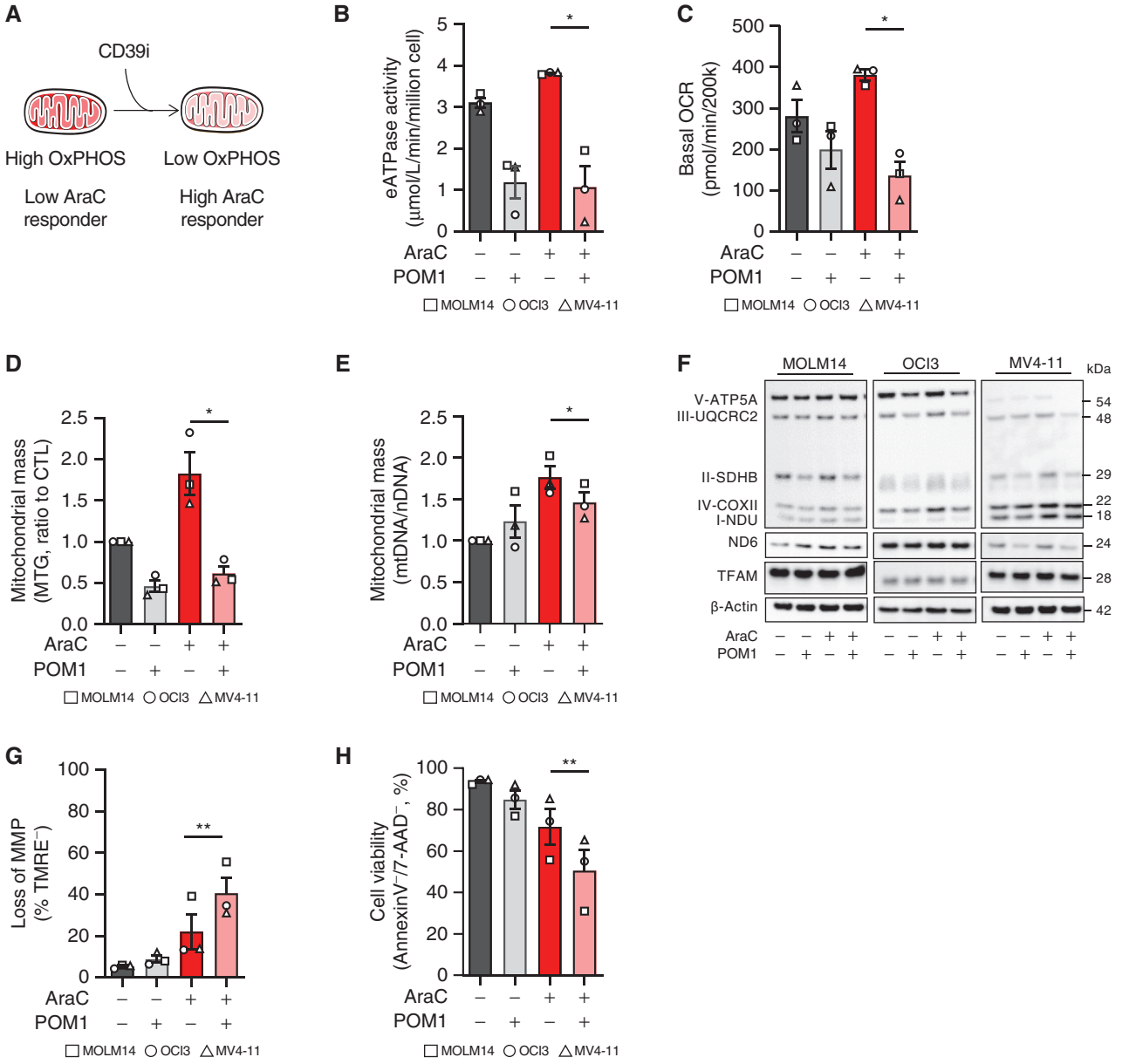

Figure 4. Effects of pharmacologic inhibition of CD39 activity on AML metabolism and response to cytarabine (AraC). **A,** Schematic depicting the metabolic reprogramming triggered by CD39 inhibition in cytarabine-resistant AML cells. **B,** eATPase activity was assessed in MOLM14, OCI-AML3, and MV4-11 after 48 hours of PBS, POM1, cytarabine, or POM-1 + cytarabine treatment *in vitro*. **C–E,** Basal OCR (**C**), mitochondrial mass (**D**), and mitochondrial DNA content (**E**) were determined in MOLM14, OCI-AML3, and MV4-11 cells cultured *in vitro* for 24 hours with PBS, POM1, cytarabine, or POM1 + cytarabine. OCR was assessed using a Seahorse analyzer (**C**). Mitochondrial mass was assessed by flow cytometry using the fluorescent MitoTracker Green (MTG), and the values were normalized to PBS-treated samples (**D**). mtDNA content was determined by real-time PCR and the quantification was based on mtDNA to nuclear DNA (nDNA) gene encoding ratio (**E**). **F,** Protein expression of the mitochondrial OxPHOS complexes in MOLM14, OCI-AML3, and MV4-11 was assessed by Western blot analysis after 24-hour treatment with PBS, POM1, cytarabine, or POM1 + cytarabine *in vitro*. **G** and **H,** Loss of mitochondrial membrane potential (MMP) was assessed following 48-hour treatment of MOLM14, OCI-AML3, and MV4-11 cells with PBS, cytarabine, POM1, and POM1 + cytarabine by flow cytometry using fluorescent TMRE probe staining (**G**). Percentage of viable cells (AnnexinV$^-$/7AAD$^-$) was measured after 48-hour treatment of MOLM14, OCI-AML3, and MV4-11 cells with PBS, cytarabine, POM1, and POM1 + cytarabine by flow cytometry using AnnexinV/7-AAD staining (**H**). *, $P \le 0.05$; **, $P \le 0.01$; ns, not significant. Histobars correspond to the mean of independent biological replicates. The number of biological replicates for each cell lines for the experiments shown in **B–E** and **G** and **H** are specified in Supplementary Fig. S8.

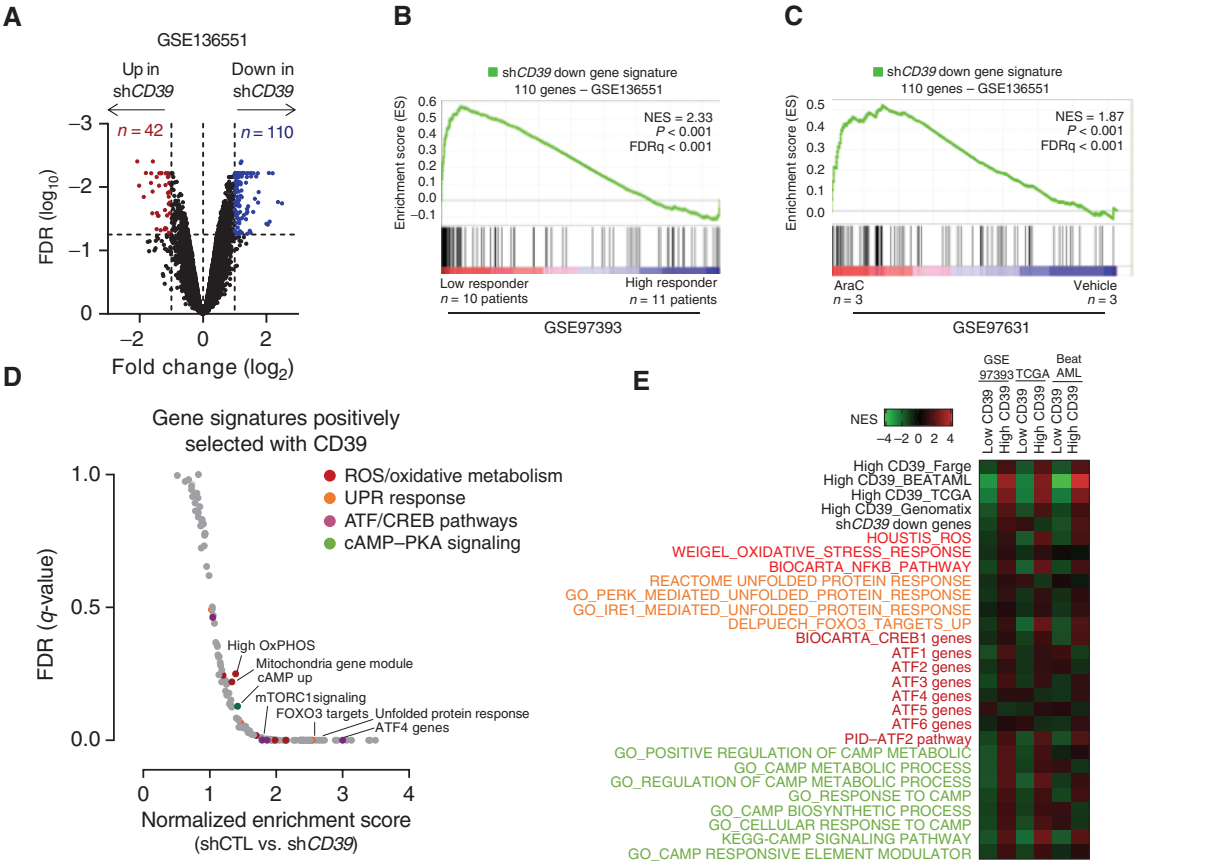

Figure 5. CD39^{hi} AML chemoresistant cells maintain an enhanced OxPHOS metabolism and support mitochondrial biogenesis through the activation of a CD39–cAMP–PKA axis. **A,** Volcano plot displaying differentially expressed genes between MOLM14 silenced for CD39 expression (sh*CD39*) and control cells (shCT). On the *y*-axis the FDR values (log_{10}) are plotted, and the *x*-axis displays the fold change (FC) values (log_2). The red dots represent the upregulated (FC > −1.0, FDR < −1.25), whereas the blue dots represent the downregulated (FC > 1.0, FDR < −1.25) expressed transcripts in sh*CD39* versus shCT MOLM14. **B** and **C,** GSEA of the sh*CD39* downregulated gene signature (*n* = 110 genes) was performed from the transcriptomes of AML patient samples characterized by poor (red) compared with good (blue) response to cytarabine (AraC) *in vivo* upon xenotransplantation in NSG mice (low vs. high responders; **B**) and from the transcriptomes of human residual AML cells purified from cytarabine-treated (red) compared with vehicle (PBS)-treated (blue) AML-xenografted NSG mice (cytarabine vs. vehicle; **C**). **D,** GSEA of the AML cell line MOLM14 shCT versus sh*CD39*. The most significantly positively enriched gene signatures are shown. The *y*-axis reports the FDR, and the *x*-axis reports the normalized enrichment score (NES) of each signature in shCTL versus sh*CD39*. Different signatures were regrouped in four larger biological process/pathway categories identified with a specific color code, as indicated in the figure. **E,** GSEA of the indicated signaling pathways gene signatures was performed on transcriptomes from patients with AML characterized by high and low *CD39* mRNA expression (the median value of CD39 expression was used as cutoff) in ref. 6 (GSE97393), the TCGA and the Beat AML cohorts. (*continued on next page*)

Altogether, our results strongly suggest that CD39 activity directly affects AML cell sensitivity to cytarabine through the regulation of mitochondrial function.

Cytarabine Residual AML Cells Display an Adaptative and Prosurvival Mitochondrial Stress Response through the Coordinated Induction of cAMP–PKA and ROS–ATF4 Signaling Downstream of CD39

Because our results strongly support the assertion that CD39 expression influences mitochondrial OxPHOS, we sought to explore signaling pathways downstream of CD39 that may promote OxPHOS metabolism and chemoresistance. Therefore, we performed targeted experiments to characterize global transcriptional changes induced by silencing CD39 (sh*CD39* vs. shControl) in the therapy-resistant MOLM14 AML cell line. A total of 152 genes were significantly and differentially expressed in MOLM14 upon silencing of CD39 [42 upregulated, 110 downregulated; log_{10} (FDR) < −1.25, log_2 (fold-change) > 1.0; Fig. 5A; Supplementary Table S2]. Consistent with our metabolic assays, gene set enrichment analysis (GSEA) indicated that CD39 loss in MOLM14 cells was negatively correlated with a gene set representing High OxPHOS function (ref. 6; NES = −1.38, FDR *q* = 0.005; Supplementary Fig. S9A). Furthermore, the sh*CD39* downregulated gene signature was significantly enriched in the transcriptomes of AML patient samples characterized by poor response to cytarabine *in vivo* in NSG (low vs. high responders, GSE97393; Fig. 5B) as well as in the transcriptomes of cytarabine-resistant AML cells from three AML PDXs (GSE97631, Fig. 5C). Gene ontology analysis of the 110 genes downregulated upon CD39 silencing indicated an enrichment in biological processes involved in cell-cycle control, DNA repair, responses to stress/stimuli, metabolism,

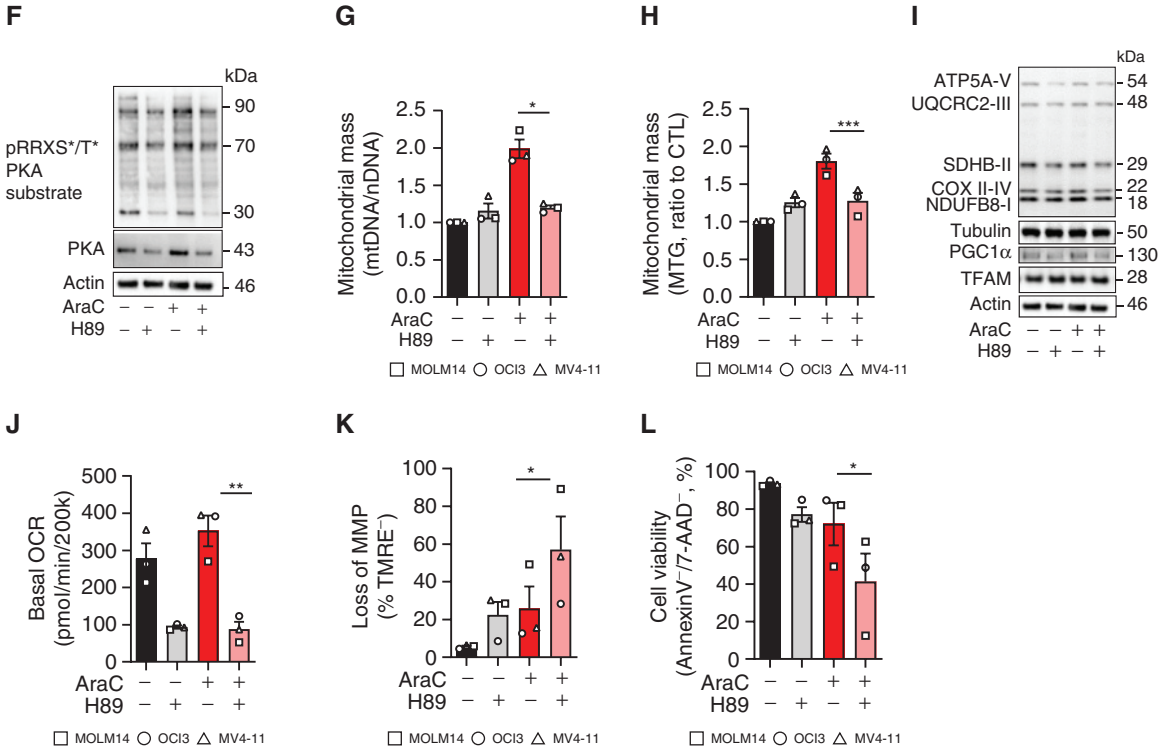

Figure 5. ***(Continued)*** **F,** Protein expression of phospho-PKA substrate (RRXS*/T*) and PKA was assessed by Western blot analysis after 6-hour treatment with cytarabine and/or H89 in MOLM14 cells *in vitro*. The housekeeping gene β-actin was used as loading control. **G,** Mitochondrial DNA content was determined in MOLM14, OCI-AML3, and MV4-11 upon treatment *in vitro* for 24 hours with PBS, H89, cytarabine, or H89 + cytarabine by real-time PCR. Quantification was based on mtDNA to nuclear DNA (nDNA) gene encoding ratio. **H,** Mitochondrial mass was assessed by flow cytometry using the fluorescent MitoTracker Green (MTG) in MOLM14, OCI-AML3, and MV4-11 cells after PBS, H89, cytarabine, or H89 + cytarabine 24-hour treatment. The values were normalized to PBS-treated samples. **I,** Protein expression of mitochondrial OxPHOS complexes, TFAM and PGC1α was assessed by Western blot analysis after 24-hour treatment with cytarabine and/or H89 in MOLM14 cells *in vitro*. The housekeeping gene α-Tubulin and β-actin were used as loading control. **J,** Basal OCR in MOLM14, OCI-AML3, and MV4-11 cells after PBS, H89, cytarabine, or H89 + cytarabine 24-hour treatment was assessed using a Seahorse analyzer. **K** and **L,** MOLM14, OCI-AML3, and MV4-11 cells were treated with PBS, cytarabine, H89, and H89 + cytarabine for 48 hours to assess (**K**) loss of mitochondrial membrane potential (MMP) by fluorescent TMRE probe and (**L**) percentage of viable cells using Annexin V/7-AAD staining by flow cytometry. *, $P \leq 0.05$; **, $P \leq 0.01$; ***, $P \leq 0.001$; ns, not significant. Histobars correspond to the mean of independent biological triplicates.

and signaling (Supplementary Fig. S9B; Supplementary Table S3). GSEA of the sh*CD39*-downregulated gene signature revealed a strong enrichment in genes involved in oxidative metabolism and reactive oxygen species (ROS) balance (FOXO3 and mTORC1 targets, among others), unfolded protein response (UPR), ATF/CREB pathway, and cAMP/PKA signaling ($P < 0.01$; Fig. 5D; Supplementary Table S4). Interestingly, all these pathways are well known to be associated with oxidative stress response and mitochondrial homeostasis. In line with this observation, transcription factor enrichment analysis identified signatures of several transcription factors playing key roles in mitochondrial function and stress response (such as ATF4/6, PARP1, and E2F1; Supplementary Fig. S9C). Next, we compared the transcriptomes of AML patient cells characterized by high CD39 expression to AML patient cells with low CD39 expression (Fig. 5E; Supplementary Fig. S7A). We confirmed a strong link between CD39 expression and the activation of mitochondrial stress response–associated pathways. On the basis of these results, we formulated the hypothesis that CD39 upregulation upon cytarabine treatment could drive an adaptative mitochondrial stress response in AML cells by inducing the coordinated activation of multiple signaling pathways regulating mitochondrial biogenesis and activity as well as ROS production and antioxidant defenses. Dynamic transcriptomic analysis of residual AML cells *ex vivo* after treatment with cytarabine revealed that the CD39 gene signature and the associated cAMP, ATF4, and FOXO3 pathways are transiently upregulated at early timepoints after chemotherapy. This simultaneously occurred when the disease reached its nadir and was subsequently downregulated between one and two weeks after the end of the treatment (Supplementary Fig. S9D–S9F). This suggests that the induction of CD39 is likely playing a key role in the initial phase of metabolic adaptation in residual AML cells.

We therefore decided to investigate the induction of oxidative stress upon cytarabine treatment and the role of CD39 in the adaptative metabolic response of AML cells to this cytotoxic stimulus. Analysis of total ROS content in CD39-high and CD39-low cellular subsets obtained from AML PDXs pretreated or not with cytarabine showed that, while the chemotherapy tended to trigger an increase in ROS, the level of CD39 expression did not affect the accumulation of ROS in AML cells (Supplementary Fig. S10A). On the contrary, the

CD39-high subset displayed a higher basal level of mitochondrial ROS in some samples, and this was maintained upon cytarabine treatment (Supplementary Fig. S10B). Next, we stratified our primary AML patient samples into ROS low and high (based on their DCF-DA staining) and we observed that ROS-high AML cells had a higher level of CD39 expression (Supplementary Fig. S10C and S10D). This suggested that, although the total level of intracellular ROS was not dependent on CD39, total ROS could affect and potentially be involved in CD39 induction in AML cells. We then investigated the role of CD39 in the regulation of ROS homeostasis as well as in the modulation of the stress response–associated ATF4 pathway in MOLM14 cells upon cytarabine treatment. Confirming previous observations in our PDXs, inhibition of CD39 did not significantly affect the accumulation of total cellular ROS triggered by the chemotherapy (Supplementary Fig. S11A). However, cotreatment with POM1 efficiently repressed the cytarabine-associated increase in mitochondrial ROS (Supplementary Fig. S11B). At the same time, cytarabine enhanced the expression of the transcription factor FOXO3a, an important regulator of mitochondrial function and antioxidant defenses, and its target mitochondrial superoxide dismutase SOD2 (but not cytosolic SOD1), as well as of the key mitochondrial stress response transcription factor ATF4. Importantly, concomitant inhibition of CD39 efficiently reversed all these effects (Supplementary Fig. S11C–S11F). We next investigated the modulation of the c-AMP–dependent PKA signaling pathway upon cytarabine treatment of MOLM14 and inhibition of CD39. Analysis of the expression and activation of key targets of the cAMP-dependent signaling pathway showed an increase in the phosphorylation of RRXS*/T*-PKA substrates upon cytarabine treatment (Supplementary Fig. S11G). These results were similar to those observed upon activation of cAMP–PKA in MOLM14 cells treated with four diverse PKA agonists (FSK, IBMX, extraATP, 8-BrcAMP), whereas treatment with PKA antagonist (H89 and PKA inhibitor 14–22 Amide PKAi) inactivated the cAMP–PKA pathway (Supplementary Fig. S11G). Finally, pharmacologic inhibition of CD39 decreased cytarabine-induced phosphorylation of RRXS*/T*-PKA substrates (Supplementary Fig. S11H). This result confirmed that CD39 activation was involved in the control of mitochondrial ROS homeostasis and redox balance, and in the activation of the mitochondrial stress–associated pathways cAMP–PKA and ATF4 upon cytarabine treatment.

To gain insight into the key pathways downstream of CD39 mediating its metabolic effects and supporting the onset of cytarabine resistance, we assessed the transcriptional and biological consequences of silencing ATF4 in MOLM14 AML cells. Notably, the si*ATF4* downregulated gene signature (100 genes) was significantly depleted in CD39-silenced AML cells and enriched in residual AML cells after cytarabine treatment *in vivo* (Supplementary Fig. S12A–S12C; Supplementary Table S5). Five transcription factors, including ATF4 itself, were commonly downregulated upon both CD39 and ATF4 silencing in AML cells (Supplementary Fig. S12D). Of note, ATF4 depletion did not significantly affect CD39 expression, supporting a role of ATF4 downstream of CD39 (Supplementary Fig. S12E and S12F). Supporting its important role in CD39-mediated acquisition of resistance to cytarabine, ATF4 genetic inactivation enhanced cytarabine-induced reduction in cell proliferation, loss of mitochondrial membrane potential, and induction of apoptosis (Supplementary Fig. S12G–S12I). However, ATF4 depletion did not have a significant impact on cytarabine-mediated increase in mitochondrial mass, the expression of ETC complex subunits and mitochondrial membrane potential (Supplementary Fig. S12J–S12L). Thus, ATF4 depletion was partially phenocopying cytarabine effects observed upon CD39 inhibition in AML cells. However, our results suggested that ATF4 did not directly contribute to the changes in mitochondrial biogenesis and function induced by CD39 in the leukemic cells exposed to chemotherapy stress.

We next investigated whether inactivation of cAMP–PKA pathway by H89, a well-known pharmacologic agent that inhibits PKA activity, could affect AML mitochondrial functions and enhance cytarabine treatment cytotoxicity similar to CD39 inhibition. As expected, H89-treated MOLM14 cells exhibited decreased levels of pRRXS*/T*-PKA substrates, including in the cytarabine setting (Fig. 5F). Importantly, the PKA-specific inhibitor H89 completely phenocopied the effect of the CD39 inhibitor POM1 on mitochondrial activity by counteracting the increase in mtDNA level (Fig. 5G), mitochondrial mass (Fig. 5H), the expression of ETC complex subunits and PGC1α (Fig. 5I), and basal OCR (Fig. 5J) induced by cytarabine treatment. Finally, H89-treated MOLM14 cells exhibited a significant loss of MMP (Fig. 5K) and decrease in cell viability (Fig. 5L). Interestingly, we noticed that the activation of PKA signaling was detectable as early as 1 hour after exposure to cytarabine in MOLM14 AML cells and peaked between 3 and 6 hours after the start of the treatment (Supplementary Fig. S13A), whereas CD39 induction was detectable only at later timepoints. Therefore, we hypothesized that the cAMP–PKA pathway could be involved in the upregulation of CD39 expression upon cytarabine exposure. In line with this, the PKA inhibitor H89 strongly repressed the increase of CD39 expression triggered by cytarabine treatment in MOLM14 cells (Supplementary Fig. S13B and S13C).

Overall, these results support a model in which cAMP–PKA signaling and the ROS–ATF4 axis act in a coordinated fashion downstream of CD39 as intrinsic pathways of resistance to cytarabine. We propose that the parallel activation of these molecular pathways orchestrates an adaptive mitochondrial stress response by regulating mitochondrial ROS production, OxPHOS biogenesis and activity, and antioxidant defenses. Moreover, our data suggest that the cAMP–PKA pathway is a key mediator of CD39-mediated effects on mitochondrial biogenesis and activity. Our results indicate that the cAMP–PKA axis acts upstream and downstream of CD39, creating a positive feedback loop, which controls and amplifies CD39-driven noncanonical intrinsic resistance pathways of adaptive stress response in AML.

The P2RY13 Purinergic Receptor Plays a Key Role in the CD39-Dependent Activation of cAMP–PKA Signaling and the Associated Metabolic Rewiring and Survival of Chemoresistant AML Cells

Having established the key role of CD39–cAMP–PKA signaling in determining the metabolic rewiring of chemotherapy-resistant AML cells, we investigated the mechanisms

responsible for the increase in intracellular cAMP upon cytarabine-linked CD39 induction. Hydrolysis of extracellular ATP into ADP and AMP by CD39 and the subsequent conversion of AMP to adenosine (ADO) by the ecto-5′-nucleotidase CD73 results in the stimulation of P1 (responsive to ADO) and P2 (responsive to ATP, ADP) purinergic X/Y receptors. This leads to modulation of intracellular cAMP and associated cAMP signaling (Fig. 6A). We therefore formulated the hypothesis that the activation of the cAMP–PKA axis was dependent on CD39-mediated increase of extracellular nucleotide levels and the associated activation of purinergic receptor signaling.

As expected, cytarabine treatment induced an increase in the production of extracellular AMP but surprisingly not ADP or adenosine in MOLM14 AML cells (Supplementary Fig. S14A). In line with our hypothesis, supplementation of exogenous ADP and AMP rescued the increase of cytarabine cytotoxic effect caused by cotreatment of AML cells with POM1 (Supplementary Fig. S14B). Interestingly, treatment of AML cell lines with the eADPase inhibitor ARL67156 (which inhibits only the CD39-mediated enzymatic conversion of ADP to AMP but not the conversion of ATP to ADP; refs. 27, 28) had only mild effects on intracellular cAMP content and did not significantly affect mitochondrial mass or activity. Furthermore, this inhibitor failed to synergistically enhance the cytotoxic effect of cytarabine compared with POM1 (Supplementary Fig. S15A–S15F). This suggested that CD39-derived eADP level was required for the activation of downstream signaling pathways that support AML metabolic rewiring and chemoresistance.

In parallel, analysis of transcriptomes from residual AML cells from PDXs with cytarabine *in vivo* highlighted a pronounced increase in the expression of the ADP-responsive G protein–coupled P2RY13 purinergic receptor concomitant with the increase of ENTPD1/CD39 expression (Fig. 6B). The increase of P2RY13 expression at the surface of residual cells upon cytarabine treatment was confirmed by flow cytometry analysis *in vitro* and *in vivo* on human AML cell lines and PDXs (Supplementary Fig. S16A and S16B). Of note, no other purinergic receptor gene was found differentially expressed in cytarabine residual AML cells compared with vehicle-treated controls (Fig. 6B). Moreover, although we occasionally observed an increase in cell surface CD73 expression upon cytarabine treatment *in vitro* in our AML cell lines, we did not observe any induction of CD73 expression *in vivo* in any of the PDXs tested after chemotherapy (Supplementary Fig. S16C and S16D). Intriguingly, we found the expression of P2RY13 and ENTPD1 to be strongly correlated in multiple AML patient datasets tested (Fig. 6C and D). Moreover, similar to the *CD39* gene signature, we found the P2RY13-associated gene signature (which we generated from the transcriptomes of patients with AML) to be highly enriched in residual AML cells upon cytarabine treatment of PDXs *in vivo* (Supplementary Fig. S16E–S16H; Supplementary Table S6). Finally, we found that CD39 and P2RY13 were concomitantly upregulated not only after cytarabine treatment, but also upon exposure to hypoxia-induced oxidative stress (Supplementary Fig. S16I). Altogether, these data indicate that these two genes might control common pathways that are critical for oxidative stress response and potentially underpin the onset of resistance to cytarabine in AML.

Indeed, cotreatment with the selective P2RY13 inhibitor MRS2211 led to a decrease in intracellular cAMP of MOLM14 AML cells *in vitro* (Fig. 6E), inhibited mitochondrial activity (measured as an increase in mitochondrial ATP production; Fig. 6F), and significantly enhanced cytarabine-dependent cytotoxic effects (Fig. 6G–I; Supplementary Fig. S16J). This partially phenocopied CD39 inhibition upon cytarabine treatment. In comparison, inhibiting adenosine purinergic signaling using an A2a adenosine receptor antagonist (ZM 241385) failed to enhance the induction of apoptosis in MOLM14 when combined with cytarabine (Supplementary Fig. S17A). Similar results were obtained by combining cytarabine treatment with an inhibitor of the 5′-ectonucleotidase CD73 (M3463, Supplementary Fig. S17B) responsible for the conversion of AMP to adenosine. Overall, these results confirm that CD39-mediated increase of extracellular nucleotide levels and the associated activation of purinergic receptor signaling underpin the activation of cAMP signaling and promote the survival of resistant AML cells upon chemotherapy treatment. In particular, our data reveal the particularly important role of CD39-mediated eADP generation and the consequent stimulation of the G protein–coupled P2RY13 receptor.

Targeting CD39 Enhances Cytarabine Chemotherapy Efficacy *In Vivo*

Our data suggest that inhibiting CD39 activity may be a promising therapeutic strategy to enhance chemotherapy response of AML cells *in vivo*. To test this hypothesis, we generated NSG mice-based CLDX and PDX models from AML cell lines and primary patient cells, respectively. We then tested the consequences of CD39 repression on the response of our preclinical models of AML to cytarabine using as alternative experimental strategies genetic invalidation and pharmacologic inhibition of our target. Genetic invalidation of CD39 was achieved in the MOLM14 CLDX model *in vivo* using two different doxycycline-inducible shRNAs specifically targeting the *ENTPD1* gene. Remarkably, CD39 depletion in combination with cytarabine treatment resulted in a significant reduction of total cell tumor burden in the bone marrow of the mice three days after the end of the chemotherapy cycle (day 18) compared with the both vehicle-treated counterparts and the shCTL-xenografted mice (Fig. 7A and B). Moreover, although no change in AML viability and loss of MMP was detectable in control MOLM14 upon cytarabine treatment, concomitant repression of CD39 triggered a significant decrease in viability and loss of MMP in AML cells (Fig. 7C and D). Altogether, this led to an enhanced cytarabine sensitivity *in vivo*, as further demonstrated by a significant increase in the overall survival of cytarabine-treated sh*CD39*-xenografted mice compared with both the vehicle-treated sh*CD39*-xenografted mice cohort and the cytarabine-treated shCTL-xenografted mice (Fig. 7E).

Pharmacologic inhibition of CD39 activity was also achieved by administering the eATPase inhibitor POM1 for 6 days at the dose of 25 mg/kg/day alone and in combination with cytarabine at 60 mg/kg/day for 5 consecutive days in two different and independent PDX models (TUH06, TUH10). Response to single and combinatory treatments and various characteristics of RLCs were specifically monitored at day 15

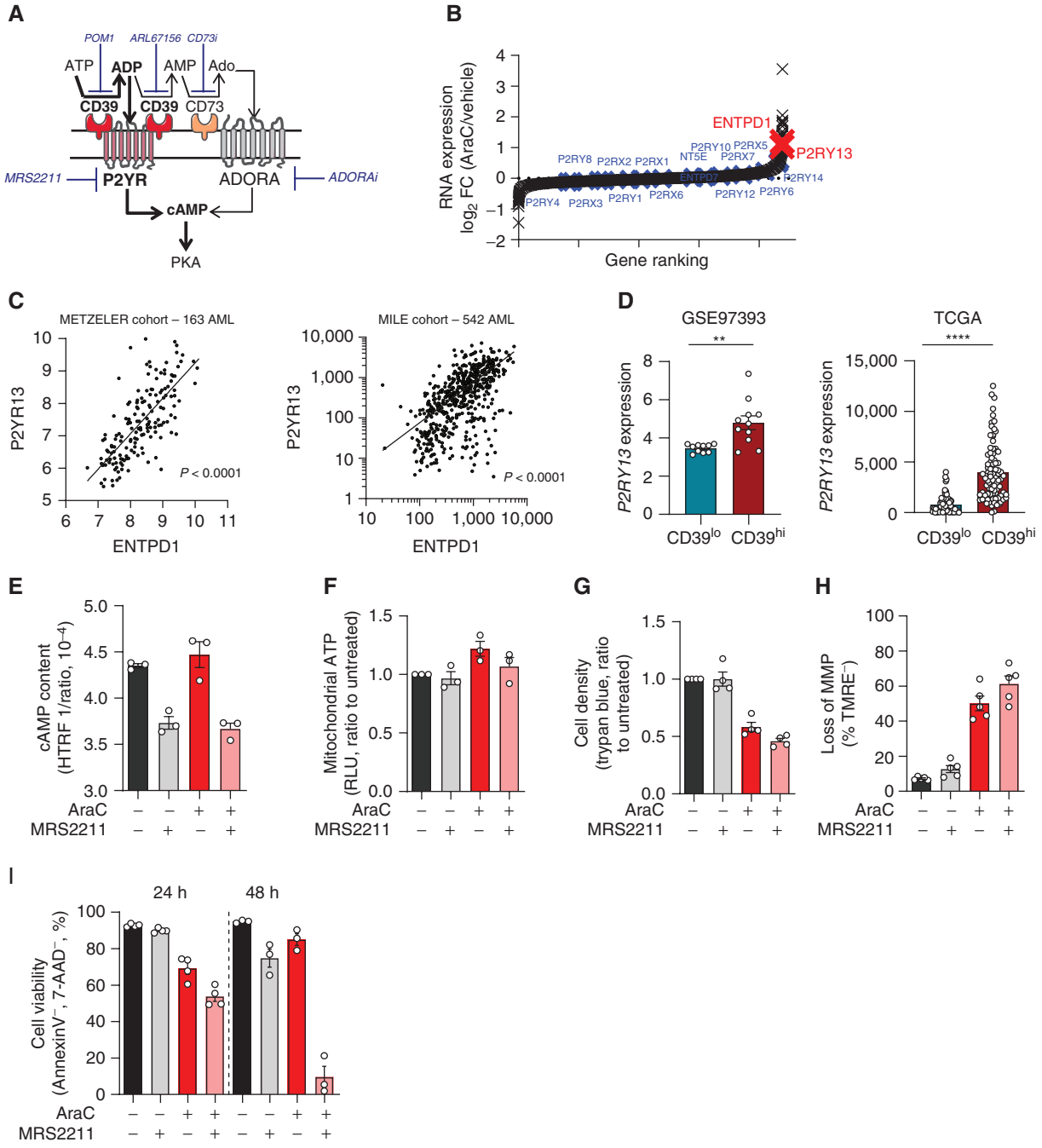

Figure 6. P2RY13 contributes through the activation of cAMP–PKA signaling to CD39-dependent metabolic changes and chemoresistant phenotype in AML. **A,** Schematic depicting the CD39–P2RY13–cAMP and CD39–CD73–Adenosine receptor (ADORA)–cAMP pathways. Highlighted in blue are the different inhibitors used in this study that act at different levels to affect these pathways. **B,** Fold-change rank plots of genes expressed in human residual AML cells purified from cytarabine (AraC)-treated versus vehicle-treated PDXs [GSE97631; cytarabine ($n = 3$) vs. vehicle ($n = 3$)]. Each cross represents one gene, and genes have been ranked on the basis of their fold change. *ENTPD1* and *P2RY13* genes are highlighted in red, whereas the genes of other purinergic receptors and ectonucleotidases are in blue. **C,** Scatter plot representing the correlation between ENTPD1 and P2RY13 expression in patients with AML from the indicated publicly available Metzeler and MILE datasets. **D,** *P2RY13* mRNA expression in AML patients subdivided by high and low CD39 mRNA expression (the median value of CD39 expression was used as cutoff) from ref. 6 (GSE97393) and the TCGA datasets. **E–I,** cAMP content (**E**), mitochondrial ATP (**F**), cell density (**G**), loss of mitochondrial membrane potential (MMP; **H**) and the decrease in cell viability (**I**) were assessed in MOLM14 cells upon treatment *in vitro* with PBS, cytarabine (1 μmol/L, **E** and **F**; 0.5 μmol/L, **G, H,** and **I**), the P2RY13 inhibitor MRS2211 (10 μmol/L, **E** and **F**; 30 μmol/L, **G, H, I**) or cytarabine + MRS2211. cAMP content was measured using the cAMP kit by Cisbio (**E**). Mitochondrial ATP production was measured using Promega Cell Titer-Glo Kit (**F**). Cell density was evaluated by cell count with trypan blue (**G**), whereas loss of MMP was assessed by flow cytometry upon staining with the fluorescent TMRE probe (**H**). The assays shown in **E–H** were performed after 24 hours of treatment. **I,** The decrease in cell viability was determined upon 24 and 48 hours of treatment using Annexin V/7-AAD staining by flow cytometry. **, $P \leq 0.01$; ****, $P \leq 0.0001$. Histobars correspond to the mean of independent biological experiments.

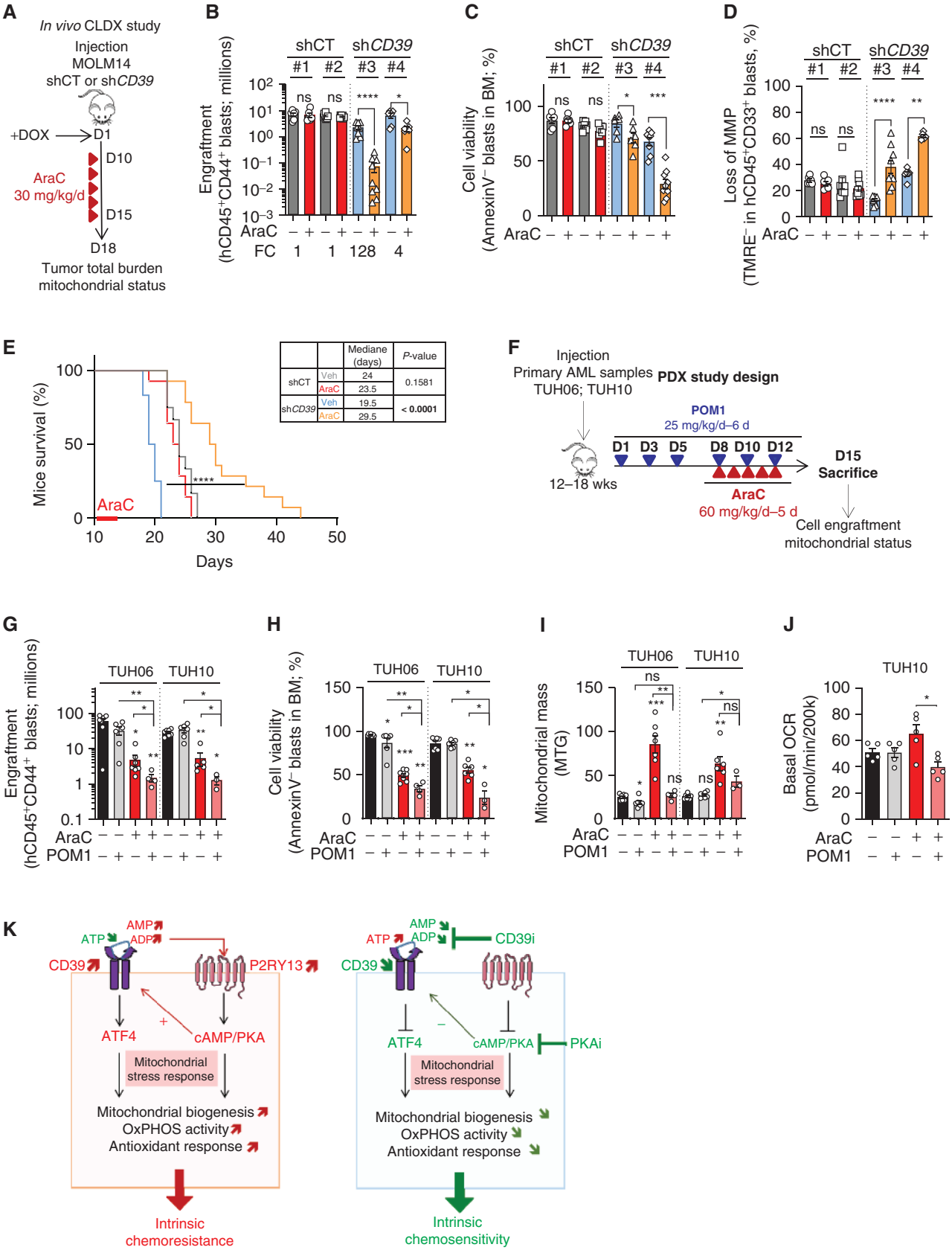

(3 days after the last administration of the combinatorial treatment; Fig. 7F). Similar to our previous results, we observed an enhancement of the cytarabine cytotoxic effect in combination with POM1 administration in all the PDXs tested with a significant reduction of the total cell tumor burden and of AML cell viability in the bone marrow *in vivo* in the combination treatment group compared with both the single treatment groups (Fig. 7G and H; Supplementary Fig. S18A and S18B). We confirmed that POM1 efficiently blocked *in vivo* the CD39 eATPase activity induced upon cytarabine treatment in two different PDX models (TUH06, TUH10; Supplementary Fig. S18C) and induced a significant reduction of the mitochondrial mass (Fig. 7I), basal and maximal mitochondrial respiration, and global energetic capacity upon the combination treatment compared with cytarabine alone (Fig. 7J; Supplementary Fig. S18D–S18G).

Notably, we did not observe an enhancement of the cytotoxic effect of the chemotherapy on healthy hematopoietic cells and progenitors in the presence of the CD39 inhibitor POM1. Indeed, the mouse CD45-positive population in the bone marrow of animals xenografted with human AML treated with the POM1/cytarabine combination did not display any decrease in viability compared with the single treatment groups (Fig. 7F; Supplementary Fig. S18H). Similarly, the combination of the CD39 inhibitor POM1 with cytarabine did not increase the sensitivity *ex vivo* of normal human $CD34^+$ hematopoietic progenitors to the chemotherapy treatment (Supplementary Fig. S18I).

Overall, our results show that inhibition of CD39 expression or activity substantially improves the response to cytarabine treatment in preclinical models of AML *in vivo* without significantly affecting the drug sensitivity of normal hematopoietic progenitors. Therefore, our findings strongly support the rationale for targeting CD39 as a valuable therapeutic strategy to enhance response to cytarabine in therapy-resistant AML. This should be assessed in a clinical study for AML treatment combining anti-CD39 small molecules with chemotherapy.

DISCUSSION

Poor overall survival is mainly due to frequent relapse caused by RLCs in patients with AML (1, 2). Although recent studies have highlighted new mechanisms of drug resistance in AML, especially *in vivo* (6, 29, 30), their clinical applications are still unresolved or under assessment. New therapies that specifically target and effectively eradicate RLCs represent an urgent medical need. In this work, we have identified the cell surface eATPase ENTPD1/CD39 and its downstream signaling pathway as a new critical and druggable target involved in the resistance to cytarabine in AML. We showed that CD39 was overexpressed in residual AML cells post chemotherapy from both 36 PDX models and 98 patients in the clinical setting. CD39 is also highly expressed in several human solid tumors, in which it was shown to actively contribute to cancer cell proliferation, dissemination, and metastatic process (31, 32). In the context of AML, our data support a model in which cytarabine treatment induces the selection and amplification of preexisting and intrinsically resistant leukemic cells that express and upregulate CD39 and its associated gene signature. We have furthermore observed that a drug-induced increase in CD39 expression is associated with a poor response to cytarabine *in vivo*, persistence of residual disease, and poor overall survival in patients with AML, especially in the younger subgroup of patients. Interestingly, our work indicates that the CD39 resistance–associated response is triggered in AML cells upon stress stimuli, such as chemotherapy, and this pathway is not necessarily constitutively activated in patients before treatment. Altogether, CD39 upregulation and downstream signaling activation play a critical role in the initial phase of responsive metabolic adaptation and regeneration of the leukemia upon chemotherapic stress. Thus, this new marker is relevant at the nadir of the disease after chemotherapy and may be useful for assessing and monitoring minimal residual disease in the clinics.

Many prosurvival and antiapoptotic signals are activated in AML by the stroma (33, 34). Nucleotides and nucleosides have emerged as important modulators of tumor biology. In particular, eATP and adenosine are major signaling molecules present in the tumor microenvironment. A growing body of evidence shows that when these molecules are released by cancer cells or surrounding tissues, they act as prometastatic factors, favoring tumor cell migration and tissue colonization. Interestingly, eATP elicits distinct responses in different

Figure 7. *In vivo* targeting of CD39 sensitizes to cytarabine in AML-engrafted mice. **A,** Schematic diagram of the chemotherapy regiment and doxycycline administration schedule used to treat CLDX NSG mice xenografted with MOLM14 transduced with shCT or sh*CD39* shRNA-expressing lentiviral vectors. The CLDX (shCTL MOLM14, sh*CD39* MOLM14) models were treated with vehicle (PBS) or 30 mg/kg/day cytarabine (AraC) given daily via intraperitoneal injection for 5 days. Mice were sacrificed 3 days posttreatment and AML cells were harvested for analysis. **B,** Cumulative total cell tumor burden of human viable $CD45^+CD44^+CD33^+$ AML cells transduced with sh*CD39* or shCT was assessed in bone marrow and spleen for the indicated groups of mice by flow cytometry. **C** and **D,** Percent of human viable AML cells (**C**) and loss of mitochondrial membrane potential (**D**) in AML cells in the bone marrow (BM) of the leukemic mice were assessed by flow cytometry using AnnexinV/7-AAD and fluorescent TMRE probe staining, respectively. **E,** The overall survival of the mice transplanted with shCTL or sh*CD39* MOLM14 cells and treated with cytarabine or vehicle as described in **A** is shown. **F,** Schematic diagram of the chemotherapy regimen and schedule used to treat NSG-based PDX (TUH06, TUH10) models with vehicle, cytarabine, or POM1 CD39 inhibitor or with a combination of the latter two. Mice were treated with the CD39 inhibitor (25 mg/kg/day) every other day for two weeks. In parallel, mice were treated with vehicle (PBS) or 60 mg/kg/day cytarabine given daily via intraperitoneal injection for 5 days. Mice were sacrificed post treatment at day 15, and the tumor total burden and the oxidative and mitochondrial status in viable AML cells was assessed. **G** and **H,** Total cell tumor burden of human viable $CD45^+CD44^+CD33^+$ AML in the bone marrow and spleen (**G**), as well as the percentage of viable human $CD45^+CD33^+$ AML cells in the bone marrow (**H**) was assessed at day 15, three days after the end of the therapy. **I–K,** The mitochondrial mass (**I**) was assessed by flow cytometry using the fluorescent probe MitoTracker Green (MTG), and the OCR (basal OCR; **J**) was assessed by seahorse in FACS-sorted human AML cells harvested from the mice at day 15, three days after the end of the therapy. **K,** Schematic diagram depicting our proposed mechanism of resistance to cytarabine involving the CD39-dependent activation of a mitochondrial stress response, regulating simultaneously mitochondrial ROS production, OxPHOS activity, and antioxidant defenses in AML cells, through the coordinated activation of the P2RY13–cAMP–PKA pathway and the ATF4 axis. *, $P \le 0.05$; **, $P \le 0.01$; ***, $P \le 0.001$; ****, $P \le 0.0001$; ns, not significant.

tumor types, ranging from promoting cancer cell proliferation (35, 36) and metastasis (36, 37) to induction of cell death (38–43). In AML, eATP was reported to reduce human leukemia growth *in vivo* and enhance the antileukemic activity of cytarabine (22). The increase of CD39 expression occurred at early timepoints of the chemotherapeutic response and residual disease processes in PDXs and patients, when its activity is likely to be potentiated by the enrichment in eATP released from apoptotic and dying cells. Bone marrow microenvironment is a key regulator of leukemia growth and can provide a chemoprotective niche for AML cells (23, 44, 45). We and others have shown that mitochondrial OxPHOS is a crucial contributing factor of AML chemoresistance, and its inhibition sensitizes cells to cytarabine treatment (6, 7, 46). This is supported by an increase in respiratory substrate availability and in mitochondrial machinery transfer from the bone marrow–derived mesenchymal stem cells (47, 48). Here we unveil an additional mechanism of resistance supporting high mitochondrial OxPHOS activity in reponse to cytarabine treatment through the enhancement of mitochondrial biogenesis and function triggered by CD39 eATPase activity.

Our work indicates that this dynamic metabolic adaptation occurs in the context of a mitochondrial stress response that is orchestrated by CD39 and involves the downstream coordinated activation of cAMP–PKA and ATF4 signaling pathways. Altogether this leads not only to the regulation of mitochondrial OxPHOS activity and ROS production, but also to the concomitant enhancement of antioxidant defenses, sustaining a prosurvival response to stress in AML cells. Indeed, CD39 inhibition strongly impaired the cytarabine-triggered increase of mitochondrial mass and mtDNA, and the upregulation of two central transcriptional regulators of mitochondrial biogenesis, PGC1α and NRF1 (49, 50). Accordingly, cotreatment with the CD39 inhibitor POM1 abrogated the increase in OxPHOS activity and mitochondrial ROS production associated with cytarabine resistance. In parallel, our results show that CD39 contributes to the upregulation of key antioxidant genes that fine-tune ROS balance and buffer the increase of mitochondrial oxidants. As evidenced by our transcriptomic analysis and confirmed by experiments of reciprocal genetic or pharmacologic inactivation, cAMP–PKA signaling and ATF4 pathway have emerged to be key downstream effectors of this CD39-driven mitochondrial stress response to cytarabine. In accordance with our findings, ATF4 has recently been reported to be a master regulator of mitochondrial homeostasis and stress response in mammalian cells (50). However, our results suggest that the activation of cAMP–PKA downstream of CD39 may be the main pathway involved in the elevation of mitochondrial biogenesis and OxPHOS activity observed in the context of AML response to chemotherapy (51, 52). In addition, the early induction of PKA signaling in AML cells upon cytarabine exposure, as well as the downregulation of CD39 upon PKA inhibition, suggest that the cAMP–PKA pathway might be acting both upstream and downstream of CD39, creating a positive feedback loop, which controls and amplifies the CD39-driven intrinsic resistance pathway through adaptive stress responses in AML.

Previous studies have reported the pleiotropic roles of cAMP signaling and its major downstream effector PKA in different cancers, including AML. Perez and colleagues showed that cAMP efflux from the cytoplasm protects AML cells from apoptosis (53). Similarly, others reported cAMP-mediated protection of acute promyelocytic leukemia against anthracycline (54) or against arsenic trioxide-induced apoptosis (55). PKA, whose activation initiates an array of transcriptional cascades involved in the immune response, cell metabolism, and mitochondrial biogenesis, is one of the main and canonical downstream effectors of cAMP signaling. Intriguingly, cAMP–PKA signaling can be localized not only at the plasma membrane or nucleus, but also at the outer mitochondrial membrane or matrix (56). Mitochondrial cAMP signaling was shown to regulate cytosol–mitochondrial cross-talk, mitochondrial biogenesis and morphology, mitochondrial dynamics, mitochondrial membrane potential, TCA cycle activities, and ETC complexes in basal and stress conditions, such as starvation or hypoxia (57). Of note, cAMP signaling is activated as an integral part of the mitochondrial stress response that allows the rewiring of cellular metabolism in the presence of cellular damage and oxidative stress conditions. In this context, PGC1α and NRF1/2 activation leads to an increase in expression and assembly of respiratory chain supercomplexes and an increase in OxPHOS activity, allowing dynamic adaptation of mitochondrial functions to survive adverse conditions (58). These studies establish a mechanistic link between cAMP, PKA, and PGC1α in the regulation of mitochondrial biogenesis/function through the activation of mitochondrial stress response.

Our data indicate that the CD39-mediated generation of extracellular ADP and AMP plays an essential role in limiting cytarabine cytotoxic effects in AML cells. In particular, eADP and its stimulation of the ADP-responsive G protein–coupled P2RY13 purinergic receptor plays an important role in the intrinsic chemoresistance function of CD39 in AML. Indeed, AML cells concomitantly increase the expression of CD39 and P2RY13 upon both cytarabine-induced cytotoxic stress and hypoxic stress. Moreover, the gene signatures associated with these two markers strongly correlate in multiple AML patient datasets tested. This suggests these two genes might control overlapping pathways underpinning the adaptation of AML cells to stress and the onset of therapy resistance. Accordingly, treatment with P2RY13 inhibitor partially phenocopied the effect of CD39 inhibition in AML cells cotreated with cytarabine. Interestingly, P2RY13 was previously reported to be involved in the protection against oxidative stress in neurons, to protect cancer cells from genotoxic stress (59, 60), and to be a potential target in AML (61). Of note, high doses of ADP induce the coupling of this purinergic receptor with G_S proteins, leading to the stimulation of adenylate cyclase and cAMP signaling (53). Treatment with P2RY13 inhibitor of AML cells resulted in a significant reduction of intracellular cAMP and inhibition of mitochondrial OxPHOS activity. This suggests that P2RY13 may be involved in the activation of the cAMP–PKA signaling downstream CD39 in AML cells upon cytarabine treatment.

Collectively, our data support a model in which CD39 eATPase activity sustains an intrinsic mitochondrial stress

response that, through the coordinated downstream activation of the P2RY13–cAMP–PKA pathway and the ATF4 axis, rewires the energetic metabolism of RLCs toward OxPHOS, and perserves their ROS homeostasis (Fig. 7K). We propose that eATP and CD39 are key actors in a novel AML cell-intrinsic mechanism of resistance to cytarabine and that targeting CD39 would be a promising therapeutic strategy to sensitize AML cells to cytarabine. In light of the recently recognized "immune checkpoint mediator" function of CD39 that interferes with antitumor immune responses, our data further suggest the existence of a critical cross-talk between AML cells and their immune and stromal microenvironment mediated by extracellular nucleotides and/or CD39 in the response to therapy of AML cells. In this context, blocking CD39 activity could have a double therapeutic benefit by both dampening the stress response and metabolic reprogramming supporting cytarabine cell-autonomous resistance and disrupting the immune escape mechanisms. In conclusion, our study uncovers a noncanonical role of CD39 on AML resistance (Fig. 7K) and provides a strong scientific rationale for testing CD39 blockade strategies in combination with cytarabine treatment in clinical trials for patients with AML. Because CD39-blocking mAbs (20, 62, 63) are already in clinical trials as a single agent and in combination with an approved anti–PD-1 immunotherapy or standard chemotherapies for patients with lymphoma or solid-tumor malignancies, we expect that these findings have the potential for rapid translation into the clinic of our proposed combination therapy targeting CD39 for patients with chemotherapy-resistant AML.

METHODS

Primary Cells from Patients with AML

Primary AML patient specimens are from Toulouse University Hospital (TUH; Toulouse, France). Frozen samples were obtained from patients diagnosed with AML at TUH after written informed consent in accordance with the Declaration of Helsinki, and stored at the HIMIP collection (BB-0033-00060). According to the French law, HIMIP biobank collections have been declared to the Ministry of Higher Education and Research (DC 2008-307 collection 1) and obtained a transfer agreement (AC 2008-129) after approval by the "Comité de Protection des Personnes Sud-Ouest et Outremer II" (ethical committee). Clinical and biological annotations of the samples have been declared to the CNIL ("Comité National Informatique et Libertés"; i.e., "Data processing and Liberties National Committee"). Peripheral blood and bone marrow samples were frozen in FCS with 10% DMSO and stored in liquid nitrogen. The percentage of blasts was determined by flow cytometry and morphologic characteristics before purification.

Purification and Culture of Cord Blood CD34$^+$ Cells

CD34-positive cells were obtained after sorting from umbilical cord blood samples (Etablissement Français du Sang, Besançon, France). Clinical and biological annotations of the samples have been declared to the CNIL. Briefly, mononuclear cells were separated by Ficoll–Hypaque density gradient centrifugation and incubated in RBC lysis buffer (ammonium chloride solution) to remove red blood cells. CD34$^+$ cell isolation was performed using manufacturer's instructions (EasySepTM, STEMCELL). CD34$^+$ samples were maintained in Iscove's Modified Dulbecco's Medium supplemented with 20% FCS.

AML Mouse Xenograft Model

Animals were used in accordance with a protocol reviewed and approved by the Institutional Animal Care and Use Committee of Région Midi-Pyrénées (France). NOD/LtSz-scid/IL-2Rγchain^{null} (NSG) mice were produced at the Genotoul Anexplo platform at Toulouse (France) using breeders obtained from Charles River Laboratory. Mice were housed and human primary AML cells were transplanted as reported previously (64–66). Briefly, mice were housed in sterile conditions using HEPA filtered microisolators and fed with irradiated food and sterile water. Transplanted mice were treated with antibiotic (baytril) for the duration of the experiment. Mice (6–9 weeks old) were sublethally treated with busulfan (20 mg/kg/day) 24 hours before injection of leukemic cells. Leukemia samples were thawed at room temperature, washed twice in PBS, and suspended in Hank's Balanced Salt Solution at a final concentration of 1–10 million cells per 200 μL of Hank's Balanced Salt Solution per mouse for tail-vein injection. Daily monitoring of mice for symptoms of disease (ruffled coat, hunched back, weakness, and reduced mobility) determined the time of killing for injected animals with signs of distress. If no signs of distress were seen, mice were initially analyzed for engraftment 8 weeks after injection except where otherwise noted.

Cytarabine Treatment In Vivo

Eight to 18 weeks after AML cell transplantation and successful engraftment in the mice (tested by flow cytometry on peripheral blood or bone marrow aspirates), NSG mice were treated by daily intraperitoneal injection for 5 days of 30 (for CLDX models) and 60 (for PDX models) mg/kg cytarabine, kindly provided by the Pharmacy of the TUH. For control, NSG mice were treated daily with intraperitoneal injection of vehicle, PBS 1×. Mice were monitored for toxicity and provided nutritional supplements as needed.

POM1 or ARL67156 was administered to xenografted mice by intraperitoneal injection every other day for two weeks. The time of dissection was fifteen days after the last dose of POM1 (or ARL67156) or 8 days for cytarabine, two days after the last dose of each treatment.

Assessment of Leukemic Engraftment

NSG mice were humanely killed in accordance with European ethics protocols. Bone marrow (mixed from tibias and femurs) and spleen were dissected in a sterile environment and flushed in Hank's Balanced Salt Solution with 1% FBS, washed in PBS, and dissociated into single-cell suspensions for analysis by flow cytometry of human leukemic cell engraftment and bone marrow cell tumor burden. Mononuclear cells from peripheral blood, bone marrow, and spleen were labeled with FITC-conjugated anti-hCD3, PE-conjugated anti-hCD33, PerCP-Cy5.5–conjugated anti-mCD45.1, APCH7-conjugated anti-hCD45, and PeCy7-conjugated anti-hCD44 (all antibodies from Becton Dickinson, except FITC-conjugated anti-hCD3 from Ozyme Biolegend) to determine the fraction of human blasts (hCD45$^+$mCD45.1$^-$hCD33$^+$hCD44$^+$ cells) using flow cytometry. Analyses were performed on a Life Science Research II (LSR II) flow cytometer with DIVA software (BD Biosciences) or Cytoflex flow cytometer with CytoExpert software (Beckman Coulter). The number of AML cells/μL peripheral blood and the cumulative number of AML cells in bone marrow and spleen (total tumor cell burden) were determined using CountBright beads (Invitrogen) following previously described protocols (6, 66).

Cell Lines and Culture Conditions

Human AML cell lines were maintained in RPMI 1640 supplemented with 10% FBS (Invitrogen) in the presence of 100 U/mL of penicillin and 100 μg/mL of streptomycin, and were incubated at

37°C with 5% CO_2. The cultured cells were split every 2 to 3 days and maintained in an exponential growth phase. U937 was obtained from the DSMZ in February 2012 and from the ATCC in January 2014. MV4-11 and HL-60 were obtained from the DSMZ in February 2012 and February 2016. KG1 was obtained from the DSMZ in February 2012 and from the ATCC in March 2013. KG1a was obtained from the DSMZ in February 2016. MOLM14 was obtained from Pr. Martin Carroll (University of Pennsylvania, Philadelphia, PA) in 2011 and from the DSMZ in June 2015. DSMZ and ATCC cell banks provided authenticated cell lines by cytochrome C oxidase I gene (*COI*) analysis and short tandem repeat (STR) profiling. Furthermore, the mutation status was also verified by targeted resequencing of a panel of 40 genes frequently mutated in AML as described in the Supplementary Methods. Clinical and mutational features of our AML cell lines are described in Supplementary Table S1. These cell lines have been routinely tested for *Mycoplasma* contamination in the laboratory.

Reagents

Cytarabine was provided by the Pharmacy of TUH. 3-Isobutyl-1-methylxanthine (IBMX), rotenone (Rot), antimycin A (AntiA), oligomycin (oligo), carbonyl cyanide 3-chlorophenylhydrazone (CCCP), sodium iodoacetate (iodo), ATP, ADP, AMP, M3763, ZM241385, and busulfan were obtained from Sigma-Aldrich. H89 and PKA Inhibitor 14–22 Amide (PKAi) were provided by Medchem Express and Calbiochem, respectively. ARL67156 (also referred to as ARL), POM1, and MRS2211 were shipped from Santa Cruz Biotechnology. 8-Bromo-cAMP and Forskolin were provided by Tocris Bioscience.

Flow Cytometry Antibodies

FITC-conjugated CD64 was provided by Beckman Coulter, and FITC-conjugated CD19, FITC-conjugated CD3, PE-Cy7-conjugated anti-hCD38, Alexa Fluor 700-conjugated anti-hCD34, APC-H7-conjugated anti-hCD45, PE-conjugated anti-hCD33, APC-conjugated anti-hCD39, PERCP-Cy5.5-conjugated anti-mCD45.1, V450-conjugated anti-hCD45 FITC-conjugated Annexin V, and BV421-conjugated Annexin V were shipped from BD Biosciences.

P2RY13 Flow Cytometry Antibody. Cells were stained during 30 minutes with anti-P2RY13 antibody (LSBIO, C120934), washed in PBS, and stained for 20 minutes with a secondary antibody–conjugated Alexa Fluor 488.

eATPase Activity Measured by Extracellular ATP Hydrolysis

5×10^4 cells treated 48 hours with different conditions (ARL 100 μmol/L or POM1 100 μmol/L) were washed and plated on 96-well plates. Plates were incubated 30 minutes at 37°C with or without ATP (10 mmol/L). The concentration of "unhydrolyzed" extracellular ATP was determined using the ATPlite luminescence ATP DetectionAssaySystem (PerkinElmer) according to the manufacturer's instructions.

Measurement of Extracellular ATP, ADP, and AMP Content

Supernatants from culture were prepared as follows: 5×10^6 cells treated 24 hours with different conditions (AraC 2 μmol/L, POM1 100 μmol/L) were washed and plated on 24-well plates. Plates were incubated 1 hour at 37°C with or without ATP (10 μmol/L). The plate was centrifuged (1,500 × *g*, −4°C, 3 minutes) and the supernatant was collected and stored at −80°C until analysis. To get highly accurate quantification, the Isotope-Dilution Mass Spectrometry (IDMS) method was applied (67). For this purpose, the day of the analysis 50 μL of IDMS standard was added to 50 μL of each sample previously diluted 2 or 20 times with water.

Analysis of ATP, ADP, and AMP supernatants was performed by high-performance anion exchange chromatography (Dionex ICS 5000+ system) coupled to a LTQ Orbitrap Velos mass spectrometer (Thermo Fisher Scientific) equipped with a heated ESI probe. All samples were analyzed in FTMS mode at a resolution of 60,000 (at m/z 400) with the following source parameters: capillary temperature was 350°C, source heater temperature was 350 °C, sheath gas flow rate was 50, auxiliary gas flow rate was 5, S-Lens RF level was 60%, and source voltage was 2.7 kV. The injection volume was 15 μL. Samples were injected on a Dionex IonPac AS11 column (250 × 2 mm) equipped with a Dionex AG11 guard column (50 × 2 mm). Mobile phase was composed of a KOH gradient which varied as follows: 0 min 0.5; 1 min 0.5; 9.5 min 4.1; 14.6 min 4.1; 24 min 9.65; 36 min 60; 36.1 min 90; 43 min 90; 43.1 min 0.5; 45 min 0.5. Data treatment was done with TraceFinder software (Thermo Fisher Scientific).

cAMP Quantification

AML cell lines were treated with medium alone or treated with ARL (100 μmol/L) or POM1 (100 μmol/L) for 6 hours; also MOLM14 sh*CD39* cells were treated with doxycycline *in vitro*. The concentration of cAMP was determined using the cAMP-Glo Assay (Promega) according to the manufacturer's instructions.

Quantification of cAMP levels was also performed using the homogeneous time-resolved fluorescence assay (HTRF) and dynamic2 cAMP kit (Cisbio). This is based on a competitive immunoassay using cryptate-labeled antibodies anti-cAMP and d2-labeled cAMP. For that purpose, M14 cells were washed and resuspended in SB1X with 0.5 mmol/L IBMX. Then, 10,000 cells/well (384-well plate) were plated and stimulated for 3 hours at room temperature with 10 μmol/L MRS2211 and 1 μmol/L cytarabine. Cells were then lysed using 5 μL of lysis buffer containing d2-labeled cAMP and 5 μL of cryptate-labeled anti-cAMP. The signal was measured after 1 hour at room temperature incubation using Artemis HTRF microplate reader. The RET signal was calculated by the ratio of d2-cAMP/cAMP Cryptate (665 nm/620 nm), the specific signal being inversely proportional to the concentration of cAMP in the sample. For each experiment, a calibration curve was established with cAMP standards allowing the quantification of cAMP levels by linear regression.

Statistical Analyses

We assessed the statistical analysis of the difference between two sets of data using nonparametric Mann–Whitney test one-way or two-way (GraphPad Prism). The Mantel–Cox log-rank test was used for statistical assessment of survival. *P* values of less than 0.05 were considered to be significant (*, $P < 0.05$; **, $P < 0.01$ and ***, $P < 0.001$).

For *in vitro* and *in vivo* analyses of cytarabine residual disease and CD39 studies, see Supplementary Methods. RNA-sequencing data are available at the Gene Expression Omnibus under the accession number GSE136551.

Disclosure of Potential Conflicts of Interest

N. Bonnefoy reports personal fees from OREGA Biotech (shareholder) outside the submitted work; in addition, N. Bonnefoy has a patent for WO2009/095478 issued and licensed to OREGA Biotech. C. Recher reports grants and personal fees from AbbVie, Astellas, Amgen, Celgene, Jazz Pharmaceuticals, Agios, Novartis, Roche, and Daiichi-Sankyo; grants from Maat Pharma and Chugai; and personal fees from Macrogenics and Pfizer outside the submitted work. No potential conflicts of interest were disclosed by the other authors.

Authors' Contributions

N. Aroua: Formal analysis, validation, methodology. **E. Boet:** Formal analysis, validation, methodology. **M. Ghisi:** Conceptualization, formal analysis, validation, writing-review and editing.

M.-L. Nicolau-Travers: Formal analysis, methodology. **E. Saland:** Formal analysis, validation, methodology. **R. Gwilliam:** Formal analysis, validation, methodology. **F. de Toni:** Formal analysis, validation, methodology. **M. Hosseini:** Formal analysis, methodology. **P.-L. Mouchel:** Formal analysis, validation, methodology. **T. Farge:** Formal analysis, validation, methodology. **C. Bosc:** Formal analysis, validation, methodology. **L. Stuani:** Formal analysis, validation, methodology. **M. Sabatier:** Formal analysis, validation, methodology. **F. Mazed:** Formal analysis, methodology. **C. Larrue:** Formal analysis, validation, methodology. **L. Jarrou:** Resources. **S. Gandarillas:** Resources. **M. Bardotti:** Resources. **M. Picard:** Resources. **C. Syrykh:** Formal analysis, validation, methodology. **C. Laurent:** Formal analysis, validation, methodology. **M. Gotanegre:** Resources, formal analysis, validation, methodology. **N. Bonnefoy:** Resources, formal analysis, validation, methodology. **F. Bellvert:** Resources. **J.-C. Portais:** Resources. **N. Nicot:** Resources, formal analysis. **F. Azuaje:** Resources. **T. Kaoma:** Software, formal analysis, validation, methodology. **C. Joffre:** Formal analysis, validation. **J. Tamburini:** Resources, formal analysis, validation. **C. Recher:** Resources, investigation. **F. Vergez:** resources, data curation, formal analysis, supervision, visualization. J.-E. Sarry: conceptualization, supervision, funding acquisition, investigation, writing-original draft, project administration, writing-review and editing.

Acknowledgments

We thank all members of mice core facilities (UMS006, ANEXPLO, Inserm, Toulouse), in particular Marie Lulka, Christine Campi, Pauline Challies, Pauline Debas, and Yara Bareira for their support and technical assistance, Cécile Déjou (Institut de Recherche en Cancérologie de Montpellier) for her help with CD39 assays, Dr. Véronique Pons and Céline Galès (Institut des Maladies Métaboliques et Cardiovasculaires de Toulouse) and Prof. Véronique De Mas and Eric Delabesse for the management of the Biobank BRC-HIMIP (Biological Resources Centres-INSERM Midi-Pyrénées "Cytothèque des hémopathies malignes") that is supported by CAPTOR (Cancer Pharmacology of Toulouse-Oncopole and Région). We thank Anne-Marie Benot, Muriel Serthelon, and Stéphanie Nevouet for their daily help with the administrative and financial management of our team. We also thank the patients and the Association GAEL for their generous support. The authors also thank Dr. Mary Selak and Laetitia Linares (Institut de Recherche en Cancérologie de Montpellier) for discussions and critical reading of the manuscript. This work was also supported by grants from the Cancéropole GSO (Projet Emergence 2014-E07, to J.-E. Sarry), Région Midi-Pyrénées/Occitanie (to J.-E. Sarry), the Programme "Investissement d'Avenir" PSPC (IMODI; to J.-E. Sarry), the Laboratoire d'Excellence Toulouse Cancer (TOUCAN and TOUCAN2.0; contract ANR11-LABEX, to J.-E. Sarry), the Programme Hospitalo-Universitaire en Cancérologie (CAPTOR; contract ANR11-PHUC0001, to C. Récher), Fondation Toulouse Cancer Santé (to J.-E. Sarry), Plan Cancer 2014-BioSys (FLEXAML; to J.-E. Sarry). N. Aroua, E. Boet, and M. Ghisi have a fellowship from the Fondation ARC, Fondation Toulouse Cancer Santé, and Fondation de France, respectively.

The costs of publication of this article were defrayed in part by the payment of page charges. This article must therefore be hereby marked *advertisement* in accordance with 18 U.S.C. Section 1734 solely to indicate this fact.

Received August 30, 2019; revised May 9, 2020; accepted July 2, 2020; published first July 8, 2020.

REFERENCES

1. Tallman MS, Gilliland DG, Rowe JM. Drug therapy for acute myeloid leukemia. Blood 2005;106:1154–63.
2. Burnett A, Wetzler M, Lowenberg B. Therapeutic advances in acute myeloid leukemia. J Clin Oncol 2011;29:487–94.
3. Vergez F, Green AS, Tamburini J, Sarry J-E, Gaillard B, Cornillet-Lefebvre P, et al. High levels of CD34+CD38low/-CD123+ blasts are predictive of an adverse outcome in acute myeloid leukemia: a Groupe Ouest-Est des Leucemies Aigues et Maladies du Sang (GOELAMS) study. Haematologica 2011;96:1792–8.
4. van Rhenen A, Feller N, Kelder A, Westra AH, Rombouts E, Zweegman S, et al. High stem cell frequency in acute myeloid leukemia at diagnosis predicts high minimal residual disease and poor survival. Clin Cancer Res 2005;11:6520–7.
5. Ishikawa F, Yoshida S, Saito Y, Hijikata A, Kitamura H, Tanaka S, et al. Chemotherapy-resistant human AML stem cells home to and engraft within the bone-marrow endosteal region. Nat Biotechnol 2007;25:1315–21.
6. Farge T, Saland E, de Toni F, Aroua N, Hosseini M, Perry R, et al. Chemotherapy-resistant human acute myeloid leukemia cells are not enriched for leukemic stem cells but require oxidative metabolism. Cancer Discov 2017;7:716–35.
7. Bosc C, Selak MA, Sarry J-E. Resistance is futile: targeting mitochondrial energetics and metabolism to overcome drug resistance in cancer treatment. Cell Metab 2017;26:705–7.
8. Vazquez F, Lim J-H, Chim H, Bhalla K, Girnun G, Pierce K, et al. PGC1α expression defines a subset of human melanoma tumors with increased mitochondrial capacity and resistance to oxidative stress. Cancer Cell 2013;23:287–301.
9. Kuntz EM, Baquero P, Michie AM, Dunn K, Tardito S, Holyoake TL, et al. Targeting mitochondrial oxidative phosphorylation eradicates therapy-resistant chronic myeloid leukemia stem cells. Nat Med 2017;23:1234–40.
10. Lee K, Giltnane JM, Balko JM, Schwarz LJ, Guerrero-Zotano AL, Hutchinson KE, et al. MYC and MCL1 cooperatively promote chemotherapy-resistant breast cancer stem cells via regulation of mitochondrial oxidative phosphorylation. Cell Metab 2017;26:633–47.
11. Henkenius K, Greene BH, Barckhausen C, Hartmann R, Märken M, Kaiser T, et al. Maintenance of cellular respiration indicates drug resistance in acute myeloid leukemia. Leuk Res 2017;62:56–63.
12. Stucki A, Rivier AS, Gikic M, Monai N, Schapira M, Spertini O. Endothelial cell activation by myeloblasts: molecular mechanisms of leukostasis and leukemic cell dissemination. Blood 2001;97:2121–9.
13. Röllig C, Ehninger G. How I treat hyperleukocytosis in acute myeloid leukemia. Blood 2015;125:3246–52.
14. Griffin JD, Rambaldi A, Vellenga E, Young DC, Ostapovicz D, Cannistra SA. Secretion of interleukin-1 by acute myeloblastic leukemia cells in vitro induces endothelial cells to secrete colony stimulating factors. Blood 1987;70:1218–21.
15. Bertoli S, Picard M, Bérard E, Griessinger E, Larrue C, Mouchel PL, et al. Dexamethasone in hyperleukocytic acute myeloid leukemia. Haematologica 2018;103:988–98.
16. de Andrade Mello P, Coutinho-Silva R, Savio LEB. Multifaceted effects of extracellular adenosine triphosphate and adenosine in the tumor-host interaction and therapeutic perspectives. Front Immunol 2017;8:1526.
17. Beavis PA, Stagg J, Darcy PK, Smyth MJ. CD73: a potent suppressor of antitumor immune responses. Trends Immunol 2012;33:231–7.
18. Bastid J, Cottalorda-Regairaz A, Alberici G, Bonnefoy N, Eliaou J-F, Bensussan A. ENTPD1/CD39 is a promising therapeutic target in oncology. Oncogene 2013;32:1743–51.
19. Bastid J, Regairaz A, Bonnefoy N, Déjou C, Giustiniani J, Laheurte C, et al. Inhibition of CD39 enzymatic function at the surface of tumor cells alleviates their immunosuppressive activity. Cancer Immunol Res 2015;3:254–65.
20. Perrot I, Michaud H-A, Giraudon-Paoli M, Augier S, Docquier A, Gros L, et al. Blocking antibodies targeting the CD39/CD73 immunosuppressive pathway unleash immune responses in combination cancer therapies. Cell Rep 2019;27:2411–25.
21. Dulphy N, Henry G, Hemon P, Khaznadar Z, Dombret H, Boissel N, et al. Contribution of CD39 to the immunosuppressive microenvironment of acute myeloid leukaemia at diagnosis. Br J Haematol 2014;165:722–5.

22. Salvestrini V, Zini R, Rossi L, Gulinelli S, Manfredini R, Bianchi E, et al. Purinergic signaling inhibits human acute myeloblastic leukemia cell proliferation, migration, and engraftment in immunodeficient mice. Blood 2012;119:217–26.
23. Tabe Y, Yamamoto S, Saitoh K, Sekihara K, Monma N, Ikeo K, et al. Bone marrow adipocytes facilitate fatty acid oxidation activating AMPK and a transcriptional network supporting survival of acute monocytic leukemia cells. Cancer Res 2017;77:1453–64.
24. Ye H, Adane B, Khan N, Sullivan T, Minhajuddin M, Gasparetto M, et al. Leukemic stem cells evade chemotherapy by metabolic adaptation to an adipose tissue niche. Cell Stem Cell 2016;19:23–37.
25. Perea G, Domingo A, Villamor N, Palacios C, Juncà J, Torres P, et al. Adverse prognostic impact of CD36 and CD2 expression in adult de novo acute myeloid leukemia patients. Leuk Res 2005;29:1109–16.
26. Grenz A, Zhang H, Hermes M, Eckle T, Klingel K, Huang DY, et al. Contribution of E-NTPDase1 (CD39) to renal protection from ischemia-reperfusion injury. FASEB J 2007;21:2863–73.
27. Durnin L, Moreland N, Lees A, Mutafova-Yambolieva VN. A commonly used ecto-ATPase inhibitor, ARL-67156, blocks degradation of ADP more than the degradation of ATP in murine colon. Neurogastroenterol Motil 2016;28:1370–81.
28. Lévesque SA, Lavoie ÉG, Lecka J, Bigonnesse F, Sévigny J. Specificity of the ecto-ATPase inhibitor ARL 67156 on human and mouse ectonucleotidases. Br J Pharmacol 2007;152:141–50.
29. Skrtić M, Sriskanthadevan S, Jhas B, Gebbia M, Wang X, Wang Z, et al. Inhibition of mitochondrial translation as a therapeutic strategy for human acute myeloid leukemia. Cancer Cell 2011;20:674–88.
30. Sriskanthadevan S, Jeyaraju DV, Chung TE, Prabha S, Xu W, Skrtic M, et al. AML cells have low spare reserve capacity in their respiratory chain that renders them susceptible to oxidative metabolic stress. Blood 2015;125:2120–30.
31. Jackson SW, Hoshi T, Wu Y, Sun X, Enjyoji K, Cszimadia E, et al. Disordered purinergic signaling inhibits pathological angiogenesis in cd39/Entpd1-null mice. Am J Pathol 2007;171:1395–404.
32. Künzli BM, Bernlochner M-I, Rath S, Käser S, Csizmadia E, Enjyoji K, et al. Impact of CD39 and purinergic signalling on the growth and metastasis of colorectal cancer. Purinergic Signal 2011;7:231–41.
33. Konopleva M, Konoplev S, Hu W, Zaritskey AY, Afanasiev BV, Andreeff M. Stromal cells prevent apoptosis of AML cells by up-regulation of anti-apoptotic proteins. Leukemia 2002;16:1713–24.
34. Zeng Z, Shi YX, Tsao T, Qiu Y, Kornblau SM, Baggerly KA, et al. Targeting of mTORC1/2 by the mTOR kinase inhibitor PP242 induces apoptosis in AML cells under conditions mimicking the bone marrow microenvironment. Blood 2012;120:2679–89.
35. Dixon CJ, Bowler WB, Fleetwood P, Ginty AF, Gallagher JA, Carron JA. Extracellular nucleotides stimulate proliferation in MCF-7 breast cancer cells via P2-purinoceptors. Br J Cancer 1997;75:34–9.
36. Janssens R, Boeynaems JM. Effects of extracellular nucleotides and nucleosides on prostate carcinoma cells. Br J Pharmacol 2001;132:536–46.
37. Wang L, Olivecrona G, Götberg M, Olsson ML, Winzell MS, Erlinge D. ADP acting on P2Y13 receptors is a negative feedback pathway for ATP release from human red blood cells. Circ Res 2005;96:189–96.
38. White N, Ryten M, Clayton E, Butler P, Burnstock G. P2Y purinergic receptors regulate the growth of human melanomas. Cancer Lett 2005;224:81–91.
39. Takai E, Tsukimoto M, Harada H, Kojima S. Autocrine signaling via release of ATP and activation of P2X7 receptor influences motile activity of human lung cancer cells. Purinergic Signal 2014;10:487–97.
40. Yokdang N, Tellez JD, Tian H, Norvell J, Barsky SH, Valencik M, et al. A role for nucleotides in support of breast cancer angiogenesis: heterologous receptor signalling. Br J Cancer 2011;104:1628–40.
41. Burnstock G, Di Virgilio F. Purinergic signalling and cancer. Purinergic Signal 2013;9:491–540.
42. Souza CO, Santoro GF, Figliuolo VR, Nanini HF, de Souza HSP, Castelo-Branco MTL, et al. Extracellular ATP induces cell death in human intestinal epithelial cells. Biochim Biophys Acta 2012;1820:1867–78.
43. Shabbir M, Burnstock G. Purinergic receptor-mediated effects of adenosine 5′-triphosphate in urological malignant diseases. Int J Urol 2009;16:143–50.
44. Lane SW, Scadden DT, Gilliland DG. The leukemic stem cell niche: current concepts and therapeutic opportunities. Blood 2009;114:1150–7.
45. Rashidi A, DiPersio JF. Targeting the leukemia-stroma interaction in acute myeloid leukemia: rationale and latest evidence. Ther Adv Hematol 2016;7:40–51.
46. Samudio I, Konopleva M. Targeting leukemia's "fatty tooth." Blood 2015;126:1874–5.
47. Moschoi R, Imbert V, Nebout M, Chiche J, Mary D, Prebet T, et al. Protective mitochondrial transfer from bone marrow stromal cells to acute myeloid leukemic cells during chemotherapy. Blood 2016;128:253–64.
48. Marlein CR, Zaitseva L, Piddock RE, Robinson SD, Edwards DR, Shafat MS, et al. NADPH oxidase-2 derived superoxide drives mitochondrial transfer from bone marrow stromal cells to leukemic blasts. Blood 2017;130:1649–60.
49. Wu Z, Puigserver P, Andersson U, Zhang C, Adelmant G, Mootha V, et al. Mechanisms controlling mitochondrial biogenesis and respiration through the thermogenic coactivator PGC-1. Cell 1999;98:115–24.
50. Scarpulla RC. Nuclear activators and coactivators in mammalian mitochondrial biogenesis. Biochim Biophys Acta 2002;1576:1–14.
51. Signorile A, Micelli L, De Rasmo D, Santeramo A, Papa F, Ficarella R, et al. Regulation of the biogenesis of OXPHOS complexes in cell transition from replicating to quiescent state: involvement of PKA and effect of hydroxytyrosol. Biochim Biophys Acta 2014;1843:675–84.
52. Yao K, Zhang WW, Yao L, Yang S, Nie W, Huang F. Carvedilol promotes mitochondrial biogenesis by regulating the PGC-1/TFAM pathway in human umbilical vein endothelial cells (HUVECs). Biochem Biophys Res Commun 2016;470:961–6.
53. Perez DR, Smagley Y, Garcia M, Carter MB, Evangelisti A, Matlawska-Wasowska K, et al. Cyclic AMP efflux inhibitors as potential therapeutic agents for leukemia. Oncotarget 2016;7:33960–82.
54. Gausdal G, Wergeland A, Skavland J, Nguyen E, Pendino F, Rouhee N, et al. Cyclic AMP can promote APL progression and protect myeloid leukemia cells against anthracycline-induced apoptosis. Cell Death Dis 2013;4:e516.
55. Safa M, Mousavizadeh K, Noori S, Pourfathollah A, Zand H. cAMP protects acute promyelocytic leukemia cells from arsenic trioxide-induced caspase-3 activation and apoptosis. Eur J Pharmacol 2014;736:115–23.
56. Di Benedetto G, Gerbino A, Lefkimmiatis K. Shaping mitochondrial dynamics: the role of cAMP signalling. Biochem Biophys Res Commun 2018;500:65–74.
57. Zhang F, Zhang L, Qi Y, Xu H. Mitochondrial cAMP signaling. Cell Mol Life Sci 2016;73:4577–90.
58. Balsa E, Soustek MS, Thomas A, Cogliati S, García-Poyatos C, Martín-García E, et al. ER and nutrient stress promote assembly of respiratory chain supercomplexes through the PERK-eIF2α axis. Mol Cell 2019;74:877–90.
59. Espada S, Ortega F, Molina-Jijón E, Rojo AI, Pérez-Sen R, Pedraza-Chaverri J, et al. The purinergic P2Y(13) receptor activates the Nrf2/HO-1 axis and protects against oxidative stress-induced neuronal death. Free Radic Biol Med 2010;49:416–26.
60. Morente V, Pérez-Sen R, Ortega F, Huerta-Cepas J, Delicado EG, Miras-Portugal MT. Neuroprotection elicited by P2Y13 receptors against genotoxic stress by inducing DUSP2 expression and MAPK signaling recovery. Biochim Biophys Acta 2014;1843:1886–98.
61. Maiga A, Lemieux S, Pabst C, Lavallée V-P, Bouvier M, Sauvageau G, et al. Transcriptome analysis of G protein-coupled receptors in distinct genetic subgroups of acute myeloid leukemia: identification of potential disease-specific targets. Blood Cancer J 2016;6:e431.
62. Young A, Mittal D, Stagg J, Smyth MJ. Targeting cancer-derived adenosine: new therapeutic approaches. Cancer Discov 2014;4:879–88.

63. Li X-Y, Moesta AK, Xiao C, Nakamura K, Casey M, Zhang H, et al. Targeting CD39 in cancer reveals an extracellular ATP- and inflammasome-driven tumor immunity. Cancer Discov 2019;9:1754–73.
64. Sanchez PV, Perry RL, Sarry JE, Perl AE, Murphy K, Swider CR, et al. A robust xenotransplantation model for acute myeloid leukemia. Leukemia 2009;23:2109–17.
65. Saland E, Boutzen H, Castellano R, Pouyet L, Griessinger E, Larrue C, et al. A robust and rapid xenograft model to assess efficacy of chemotherapeutic agents for human acute myeloid leukemia. Blood Cancer J 2015;5:e297.
66. Sarry JE, Murphy K, Perry R, Sanchez PV, Secreto A, Keefer C, et al. Human acute myelogenous leukemia stem cells are rare and heterogeneous when assayed in NOD/SCID/IL2Rγc-deficient mice. J Clin Invest 2011;121:384–95.
67. Wu L, Mashego MR, van Dam JC, Proell AM, Vinke JL, Ras C, et al. Quantitative analysis of the microbial metabolome by isotope dilution mass spectrometry using uniformly 13C-labeled cell extracts as internal standards. Anal Biochem 2005;336:164–71.